UNIVERSITY OF TWENTE.

**Faculty of Electrical Engineering,
Mathematics & Computer Science**

Tracking and Control of Soft, Self-folding Miniaturized Agents using Ultrasound Images

Krishna Kumar Thirukokaranam Chandrasekar

Master Thesis Report
September 2016

Supervisors:
Dr. Gwenn Englebienne
Dr. Mannes Poel
Dr. Stefano Scheggi

Human Media Interaction Group
Faculty of Electrical Engineering,
Mathematics and Computer Science
University of Twente
P.O. Box 217
7500 AE Enschede
The Netherlands

Declaration of Authorship

I, Krishna Kumar, declare that this thesis titled, *'Tracking and Control of Soft, Self-folding, Miniaturized Agents using Ultrasound Images.'* and the work presented in it are my own. I confirm that:

- This work was done wholly or mainly while in candidature for a research degree at this University.
- Where any part of this thesis has previously been submitted for a degree or any other qualification at this University or any other institution, this has been clearly stated.
- Where I have consulted the published work of others, this is always clearly attributed.
- Where I have quoted from the work of others, the source is always given. With the exception of such quotations, this thesis is entirely my own work.
- I have acknowledged all main sources of help.
- Where the thesis is based on work done by myself jointly with others, I have made clear exactly what was done by others and what I have contributed myself.

Signed: _____

Date: _____

"The Beliefs you hold in the beginning of the Journey Defines the Journey"

-Anonymous

UNIVERSITY OF TWENTE

Abstract

Human Media Interaction
University of Twente

Master of Science

Tracking and Control of Soft, Self-folding Miniaturized Agents using Ultrasound Images.

by Krishna Kumar

The usage of micro-sized agents in magnetic based drug delivery systems could be made a lot more affordable if it is possible to control these agents wirelessly based on feedback obtained from the ultrasound clinical images. However, since the image is of ultrasound type, the most common edge detection techniques used in digital image processing has to be modified and adapted in such a way, the control of the micro agent is made possible. The main reason is due to absence of sharp edges with the obtained image. The thesis mainly focuses on solving this problem. Also Control algorithms were written to control and drive the robot across various scenarios and motion profiles for performing pick and move operations.

Thus the goal of this assignment is to track and control hydrogel micro-grippers using two-dimensional ultrasound images. In the initial step a tracker is designed which is evaluated with the collected datasets. The tracker is then implemented to detect the miniaturized gripper and to track it in the presence of occlusions. Following it, an experimental validation of the proposed technique is performed. After the evaluation, the proposed algorithm is used in the experimental setup to control the motion of the miniaturized agent along a defined path. Various motion experiments were performed in order to evaluate the performance of the proposed technique. Finally, with the help of proper motion profiles and control algorithms, the hydrogel gripper is made to reach a bead, grasp it and transport it to a specified target area.

Also in order to evaluate clinically relevant scenarios, algorithms and advanced computer vision techniques were selected and compared for exploring the best possible features from the ultrasound images and eventually based on the results, a specialized tracker was formulated with aim of tracking the micro gripper in real tissue type of environment.

Acknowledgements

Foremost, I would like to express my sincere gratitude to Prof. Dr. Sarthak Misra and my daily coordinator Dr. Stefano Scheggi for providing me the opportunity to be part of and write my Master thesis with the Surgical Robotics Lab, University of Twente. Their continuous support throughout the research, with utmost patience and motivation helped me immensely in successfully completing the research.

Besides my coordinator, I would like to thank my advisor and mentor Dr. Gwenn Englebienne for his constant guidance, encouragement, insightful comments, and hard questions that was extremely helpful in shaping my thesis in the right direction. I could not have imagined having a better advisor and mentor for my master study. I would like to thank Dr. Mannes Poel, whose guidance helped me shape up this report really well.

I thank my fellow labmates in surgical robotics lab: Dr. Alper, Fedrico, Gert, Jacob, Pedro and Hassna, for the stimulating discussions, for the sleepless nights we were working together before deadlines, and for all the fun we have had in the last six months.

Also I thank my friends: Aishwarya, Thaya, Ramya, Sai, Bhuvi, Sathya, Santy, Vijay, Gowri, Deepa, Sharan, Bala, Akshaya, Nithin, Kristijan, Dan and Karthick who all make me what I am today. In particular, I am grateful to Thaya for constanly motivating me whenever required, who was also instrumental in making me believe what I am capable of.

Last but not the least, I would like to thank my family: my sister Roshni for being there for my all the time and my parents Chandrasekar and Shyamala, for giving birth to me at the first place and supporting me spiritually throughout my life.

The research leading to these results has received funding from the Netherlands Organization for Scientific Research (NWO) Innovative Medical Devices Initiative (IMDI) - Project: USE (Ultrasound Enhancement) and from the Eu- ropean Unions Horizon 2020 Research and Innovation Pro- gramme - Project: ROBOTAR (Grant Agreement 638428).

Contributions

1. Stefano Scheggi, Krishna Kumar .T. Chandrasekar, ChangKyu Yoon, Ben Sawaryn, Gert van de Steeg, David H. Gracias and Sarthak Misra, "*Magnetic-Based Motion Control and Planning of Hydrogel Grippers using Ultrasound Images"* Robotics and Automation (ICRA), 2017, IEEE International Conference, Marina Bay Sands, Singapore. - *Submitted (in for peer review)*

Contents

List of Figures

Abbreviations

US	**U**ltra **S**ound
PID	**P**roportional **I**ntegral **D**erivative
HoG	**H**istogram **O**f **G**radients
HG	**H**ypothesis **G**eneration
HV	**H**ypothesis **V**erification
SIFT	**S**cale **I**nvariant **F**eature **T**ransform
RoI	**R**egion **O**f **I**nterest

Physical Constants

Speed of Light $c = 2.997\ 924\ 58 \times 10^8\ \mathrm{ms}^{-\mathrm{S}}$ (exact)

Symbols

D	diameter	mm
$\dot{P}$	linear velocity	m/s^2
$B(P)$	Magnetic Field	
I	current	A
α	rotational drag coefficient	Am^2sT
$\wedge$	Force - current map	

For/Dedicated to/To my...
Family & Friends

Chapter 1

Introduction

Robotic minimally invasive surgery aims to benefit medicine by improving clinical outcomes, minimize patient trauma, and enable treatment of inoperable patients. In particular, micro-sized agents can benefit robotic minimally invasive surgery since they can be inserted into the human body and use natural pathways such as arteries and veins or the gastrointestinal tract, to reach their target for drug delivery or diagnosis.

Since micro-robots can be controlled with high precision they are also interesting for micro-manipulation tasks. Micro-robots can be used as carriers for transportation and assembly at micro-scale. Sanchez *et al.* demonstrated micro-manipulation with micro-robots by using catalytic micro-bots for transportation of animal cells to desired targets [9]. Furthermore, clusters of micro-particles and swarms of flagellated bacteria [10], [11] have been demonstrated to perform micro assembly tasks. The above mentioned micro-robots are scarce in option since their ability is limited only to push and move objects while performing trivial micro-manipulation tasks. On the other hand, agents with the ability to grip, provide significant advantages in achieving complex tasks. Precise micro-assembly, targeted drug delivery (as the drug can be released), biopsy (tissue sample can be grabbed), micro-manipulation (objects can be grabbed and delivered at a target location), minimally invasive surgery, genetics, cell manipulation and mechanical characterization are few of the application that has been made possible by the use of small scale shaping changing micro grippers [5]-[8].

Recent advancements in chemical and bio-molecular engineering allowed us to produce micro-robots with shape-changing and gripping capabilities, thus providing significant advantages in achieving complex manipulation tasks. Such grippers with grabbing functionality have been used in *in vivo* experiments [12]-[14], however they are relatively large (cm scale). Down-scaling is a challenge and in order to overcome this problem, Gracias *et al.* introduced self-folding grippers based on capillary forces, thin film stress

mismatch, and swelling [15]-[18]. These grippers consist of different layers which either expand or contract, based on temperature or pH-levels eventually leading the gripper to either open or close. It also makes it essential for the grippers to be safe enough to navigate through our body without damaging any tissues. Therefore for this study we make use of grippers that are made from soft, bio-degradable, safe material. The soft grippers are made of shape changing material, hydrogel paired with a rigid non-swelling polymer that are patterned with iron-oxide. Hydrogel is a soft bio- degradable material which changes volume with changing temperature. The bio-degradable swelling property of the hydrogel, along with its ferro-magnetic property, makes it the best pick for gripping purposes.

The usage of micro-sized agents in magnetic based drug delivery systems could be made a lot more affordable if it is possible to control these agents wirelessly based on feedback obtained from a clinically viable imaging modality. MRI and ultrasound are the most commonly used clinical imaging modalities. Magnetic Resonance Imaging (MRI) has been used in the previous researches to detect and control magnetic drug carriers, nano-robots, and magnetotactic bacteria [19],[20]. However, a major drawback in using the MRI based tracking and actuation is the possibility of a delay being induced due to communications between the various modules of the interventional platform. For a bio-medical application, it is highly essential to have a real time tracking and realization of control and such a time delay, could cause instability in the closed loop control system. On the other hand, ultrasound (US) is one of the few cost efficient imaging modalities that has been used in the healthcare diagnostic industry for a long time, that could be used as an effective replacement for the camera. Factors like safe, positive effects to human health, adequate resolution and high frame rates, makes US a favorable choice [21]. However, if the image is of ultrasound type, the most common detection techniques used in digital image processing has to to be modified and adapted in such a way, control of the micro agent is made possible. It is mainly due to absence of sharp edges with the obtained ultrasound image. The thesis mainly focuses on solving this problem. Also Control algorithms were written to control and drive the robot across various scenarios and motion profiles for performing pick and move operations.

Thus the goal of this assignment is to track and control miniaturized hydrogel grippers using ultrasound images. The first part of the thesis evaluates the performance of the gripper in performing pick-and-move tasks. The gripper is controlled using the feedback from ultrasound images. The grippers are employed and evaluated across different motion profiles and autonomously maneuvered to reach the target position avoiding simulated static obstacles. The grippers were also used as carriers for pick-and-move of a polystyrene micro-bead. These experiments demonstrate the soft nature, grabbing and positioning capabilities of the grippers and control abilities of ultrasound

image guided magnetic system. Furthermore these experiments also demonstrate the magnetic systems tracking, positioning and thermal control capabilities.

The second part of the thesis is dedicated for the investigation of a tracker model that could be used to detect and track the gripper inside the human body. This is the first attempt to investigate and propose a tracker to track a miniaturized agent in real tissue environment. In order to evaluate such clinically relevant scenarios, algorithms and advanced computer vision techniques are selected and compared for exploring the best possible features that can be obtained from the ultrasound images. This eventually led to the proposal of a specialized tracker that was formulated with aim of tracking the miniaturized gripper in a real tissue environment. For this purpose, synthetic datasets were developed from real tissue samples and the tracker was trained and tested with those datasets.

The thesis report is organized as follows: Chapter 2 presents the necessary background knowledge that is required for a better understanding of the study. Chapter 3 is paper that presents the results of the grippers in performing pick and move operation that is controlled using ultrasound images. Chapter 4 presents the initial results and idea towards a sophisticated tracker that could be used for tracking the miniaturized gripper in real tissue medium. Then follows Chapter 5 that discusses the overall results and contributions of the thesis. The report finally concludes with the conclusion chapter.

Chapter 2

Background Introduction

The small scale untethered robots has been proven to be used in a broad variety of applications, such as manipulation, assembly and micro-actuation [2]-[4]. However, these traditional small robots are often passive with no shape-changing capabilities. This limits the robots in performing complex challenging tasks. On the other hand, agents with the ability to grip, provide significant advantages in achieving complex tasks. Precise micro-assembly, minimally invasive surgery, genetics, cell manipulation and mechanical characterization are few of the application that has been made possible by the use of small scale micro grippers [5]-[8]. For instance, Gultepe *et al.* demonstrated the feasibility of an *in vivo* biopsy of the porcine bile duct using thermally-responsive grippers [22]. Ichikawa *et al.* demonstrated the enucleation of bovine oocytes using untethered millimeter-scale grippers [7].

Size reduction and untethered actuation are critical to enable maneuverability of small-scale grippers in hard-to-reach environments. Conventional robotic approaches with electrical motors and actuators do not allow for significant miniaturization of the electronic components and on-board batteries. Hence, the use of wirelessly powered self-folding robots have drawn interest and shown promising results [23]-[29]. A family of prominent self-folding structures are composed of hydrogels that have several attractive properties of relevance to untethered small robots. Many grippers can be constructed with bio-compatible and even bio-degradable polymer chains or cross-linkers making them attractive for biomedical applications. They can function in aqueous media of relevance to biology and medicine. Their soft and squishy nature allows them to mimic the touch and feel of biological and even human appendages. Finally, they can be photopatterned into definite shapes so that they can change their shape on swelling and shrinkage [30].

2.1 Soft, untethered, Miniaturized grippers

In this research, we used and exploited such soft, untethered, miniaturized gripper that have magnetic and shape changing characteristics to transport micro-sized objects with an aim of using them in drug delivery systems and in performing clinical biopsies. A stiff polymer (SU-8) in combination with the hydrogel is used for achieving self-folding. As previously demonstrated, microtools, that could have significant strength and capability to be used in grasping applications, could be created using the combination of the stiff polymer and reversibly swelling hydrogel. In a related study, open-loop control of soft grippers was demonstrated by Breger *et al.*, who doped the polymer with magnetic nano-particles [31]. We utilize similarly designed grippers to realize closed-loop control and obtain greater levels of precision and reliability that are not achievable in open-loop. Fusco in *et al.* [25], [26] has also reported the closed-loop control of the hydrogel grippers. The main differences between [25], [26] and our study are: (a) In [25], [26], the magnetic control was possible only when a magnetic object was gripped, since the grippers used were not magnetic themselves; (b) Previously near-IR radiation was used to heat the grippers whereas here we use a Peltier element; (c) The accuracy of previously reported tasks remains unclear since the numerical results and analysis of the closed-loop motion control and pick-and-move tasks were not reported whereas we have recorded, analysed and reported all the results for the closed-loop controlled motion experiments.

In the following subsections, the main characteristics of the miniaturized gripper, which are exploited in our experiments to fulfill the tasks, are explained in detail. We begin the explanation with the fabrication of the miniaturized grippers followed by explaining their magnetic and thermal characteristics.

2.1.1 Fabrication of Miniaturized Grippers

The fabrication process of the segmented SU-8 continuous *poly-N-isopropylacrylamide (pNIPAM-AAc)* bilayer grippers begins with the spin coating of hydrolyzed polyvinyl alcohol (PVA)[90%] sacrificial layer onto a silicon (Si) wafer, which is baked for 5 minutes at 115° C (Fig. 2.1). SU-8 is then spin coated on the PVA at 2000 rpm followed by a pre-bake process at 70° C for 1 minute, 115° C for 3 minutes, and 70° C for 1 minute. In order to formulate crosslinking, 21 μm-thick photopatterned SU-8 film is exposed to 180 mJ/cm2 365 nm ultraviolet (UV) light. Following the crosslinking, the post-baking process is initiated at 70° C for 1 minute, 115° C for 3 minutes and 70° C again for 1 minute. Commercial SU-8 developer is used for 1 minute and is washed with acetone and isopropyl alcohol for a few seconds and finally dried using compressed air to remove uncrosslinked portions of the SU-8. To make the 34 μm- thick magnetic second layer,

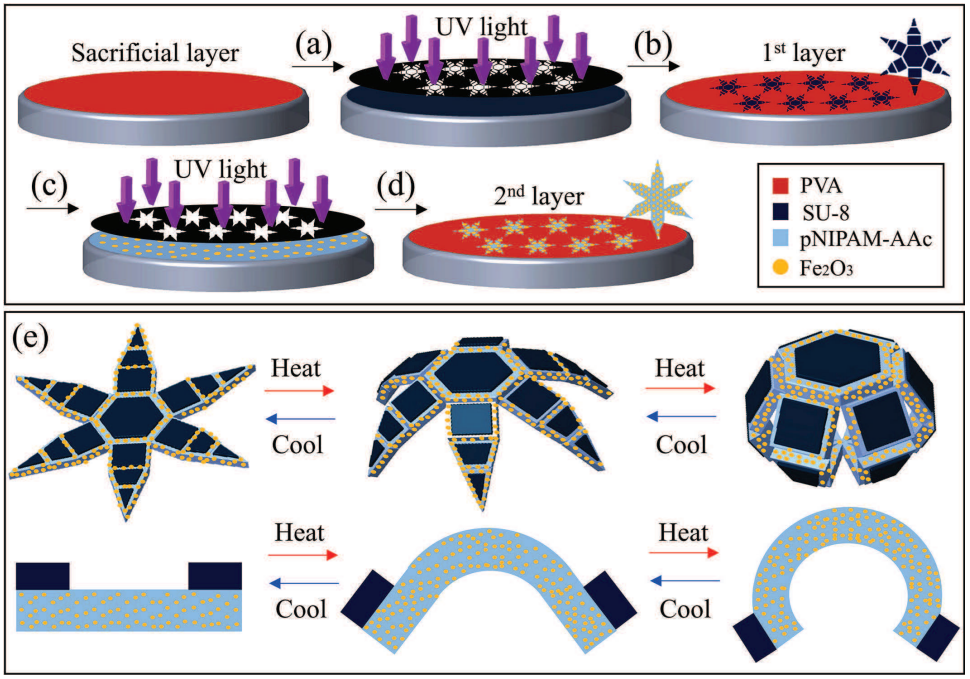

FIGURE 2.1: The schematic explaining the fabrication process of the micro grippers. SU-8 is spin-coated on a polyvinyl alcohol (PVA) sacrificial layer.(b) The SU-8 film is photopatterned and exposed to ultraviolet (UV) light. (c) A 95% poly- N-isopropylacrylamide (pNIPAM-AAc) and 5% bio-compatible Fe2O3 layer is deposited on the SU-8 layer. (d) The coated surface is photopatterned and exposed to UV light to obtain segmented, multi-fingered, bilayer grippers with rigid phalanges and flexible joints. (e) Schematic images of the untethered grippers in open and closed (grasping) configurations. Also shown is a side-view of a single hinge.[1]

pNIPAM-AAc stock solution is made of 5% w/w bio-compatible iron (III) oxide (Fe2 O3, Sigma-Aldrich, St. Louis, USA) 50 nm nanoparticles [31]. This synthesised pNIPAM-AAc solution is patterned on the previously photopatterned SU-8 segments using a second dark field mask that is oriented in non-contact mode using spacers. Following the depositing and alignment process, pNIPAM-AAc is subjected to an exposure of 40 mj/cm2 UV light that initiates cross linking. Before drying using compressed air, the acetone and IPA wash is repeated to remove uncrosslinikings. The PVA sacrificial layer is dissolved by immersing the the final wafer in DI water overnight. The grippers have an hexagram shape with a tip-to-tip diameter of 4 mm when fully open. When fully closed, the gripper becomes sphere shaped with a diameter of 0.4 mm diameter.

2.1.2 Magnetic Characterization of miniaturized Grippers

The grippers are characterised based on the result of the fabrication process evaluation for their magnetic dipole moment and thermal behaviour. The entire control model of the proposed system is based on the magnetic dipole moment of the grippers ($\mathbf{mg} \in \mathbb{R}^{\mathbf{3\times 1}}$). Now it makes it essential for us to evaluate the **mg**, for which we consider

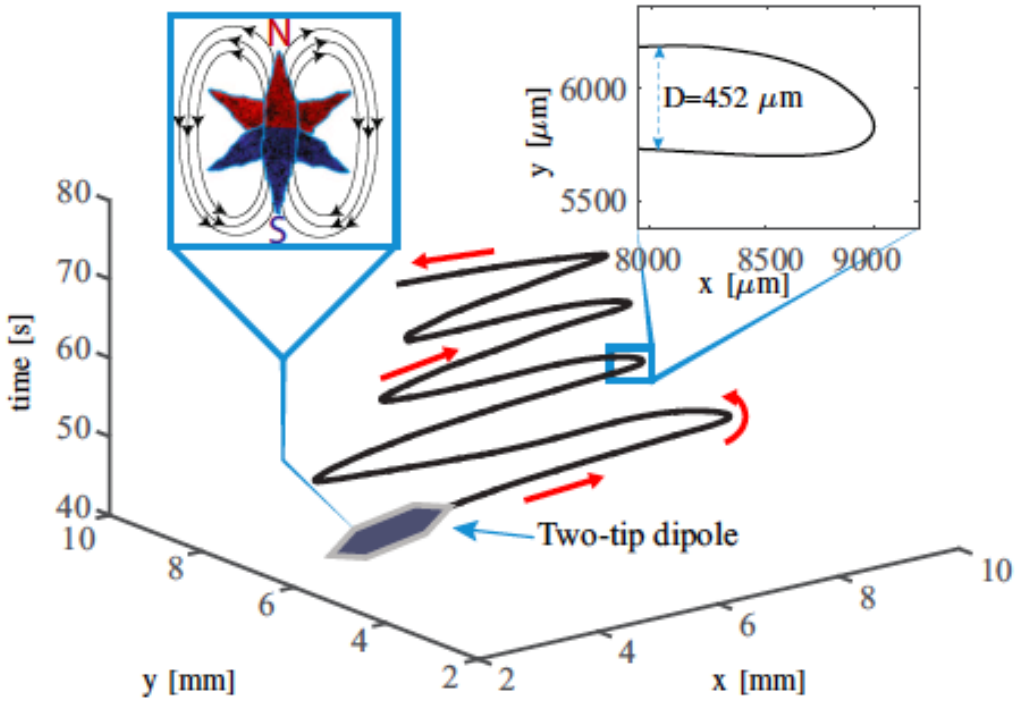

FIGURE 2.2: The figure denotes the U-turn experiment and the corresponding trajectories of the two-tip dipole. *Left inset*: shows the graphical representation of the magnetic dipole moment in regards to the two tip dipole moment.

that the grippers have a uniform Fe_2O_3 distribution. Now we have a six tip gripper and thus divide them into three pairs of counter posed two-tip dipoles. Now the magnetic dipole moment of the separate pairs ($\mathbf{m_{tips}} \in \mathbb{R}^{\mathbf{3\times1}}$) can be superimposed to calculate mg. The magnitude of the $\mathbf{m_{tips}}$ can be experimentally measured using the U-turn technique, by removing four tips from the gripper to obtain a **two-tip** dipole [34]. The **two-tip** dipole would force itself to align the magnetic field lines and reversing the field direction suddenly, would cause them to make a U-turn whose diameter (D) is given by

$$\mathbf{D} = \frac{\alpha\pi|\dot{\mathbf{P}}|}{|\mathbf{m_{tips}}||\mathbf{B(P)}} \tag{2.1}$$

where $\dot{\mathbf{P}} \in \mathbb{R}^{\mathbf{3\times1}}$ is linear velocity of the dipole, and α is its rotational drag coefficient. The value of α is calculated to be 2.2×10^{-11} Am^2sT which approximates the **two-tip** dipole by a cylinder [35]. To estimate the dipole moment, an uniform magnetic field of 3.5 mT is applied. U-turn is then initiated by reversing the fields. This process is repeated for over 20 times. The average U-turn diameters and velocity as calculated from the experiments are 0.19 ± 0.05 mm and 0.73 ± 0.13 mm/s, respectively. Using the equation 1, $|\mathbf{m_{tips}}|$ is obtained, which is equal to 3.5×10^{-8} Am2. The direction of $\mathbf{m_{tips}}$ is determined using $\mathbf{m_{tips}} = \mathbf{pd} = |\mathbf{m_{tips}}|\frac{\mathbf{d}}{|1|}$ where $\mathbf{p} \in \mathbb{R}$ is the magnetic pole strength and $\mathbf{d} \in \mathbb{R}^{\mathbf{3\times1}}$ is the vector separating the two poles [36]. Finally the superposition of

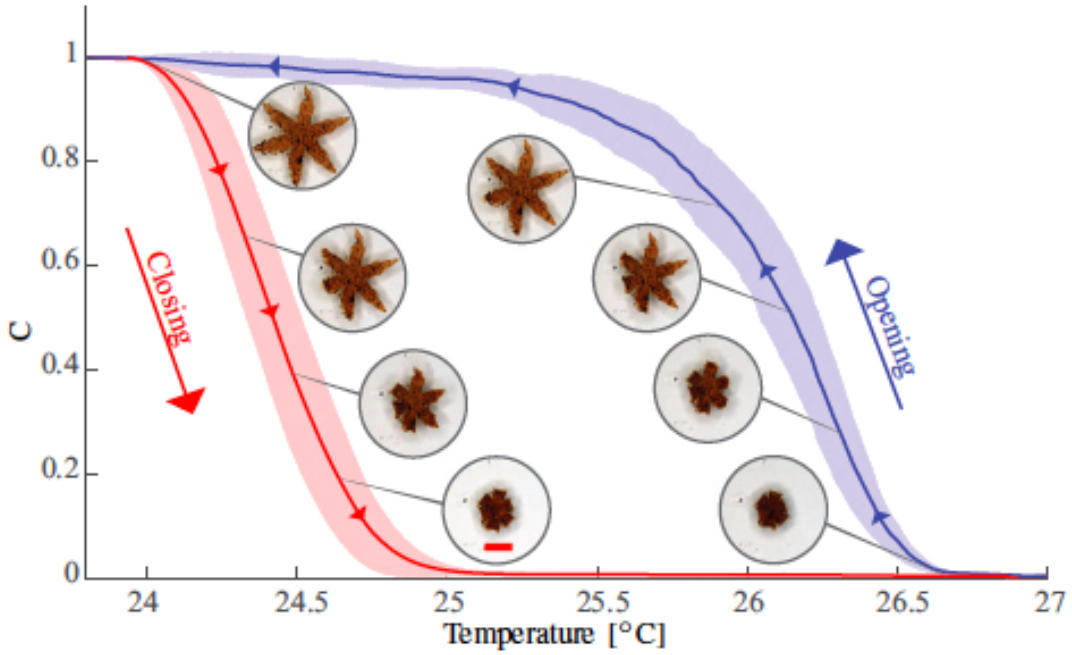

FIGURE 2.3: Results of the opening and closing characterization of the soft grippers (15 experimental trials): The red and blue lines show the average configuration of the grippers when they are heated and cooled, respectively. The corresponding shaded areas depict the standard deviations. The coefficient C is an indicator of the configuration of the grippers and varies from 1 (for an open configuration) to 0 (for a closed configuration). The value is computed as $C = \frac{D(T)-D_{closed}}{D_{open}-D_{closed}}$, where D(T) is the diameter of the contour of the gripper at temperature T, $D_{closed}$and D_{open} are the diameter values for the completely closed and open gripper, respectively. The scale bar is 0.8 mm.

three rotated two-tip dipoles is used to calculate the magnetic dipole moment of the gripper. The orientation in comparison to gripper is shown in figure (Fig. 2.2) while the **mg** was computed as 7×10^{-8} Am2. It was also evident that the magnetic dipole moment of the central part was overestimated by this method. But since the **d** is small, this portion has minimal effect on the overall magnetic dipole moment.

2.1.3 Thermal Characterization

For the purpose of exploiting the grippers for manipulation tasks, it is essential to study and characterize the thermal response of the gripper, that attributes to its shape changing abilities. In order to close the gripper the temperature of the water was increased until the gripper closes completely, and the temperature was reduced to room temperature to open it back. In this process, the star shaped gripper changes its shape gradually and becomes a sphere when completely closed and again back to star shaped when open (Fig. 2.3). The configuration of the gripper is therefore evaluated using the diameter of the gripper. The above explained closing and opening cycle experiments

was repeated for a fixed number of times for many different grippers and the analyzed results are as shown in Fig. Based on the results, the grippers were completely open below 24°C and were fully closed above 27°C. As shown in (Fig. 2.3), we were also able to find a variance in the boundaries which was mainly due to the temperature dynamics. One other interesting characteristic is that the open grippers closed at a temperature lower than the same gripper when closed, open. This due to the fact the heating rate was attributed to be higher than the cooling rate.

2.2 Ultrasound Imaging

The Ultrasound (US) is one of the most predominately used imaging modalities in medical diagnostics procedures. The theory behind the working principles of the US is almost similar to a SONAR. A concentrated and calculated frequency of the sound wave is focused onto the target, and based on the properties of the target object, certain parts of the sound wave are reflected back. This reflected sound wave carries necessary information that is used to reconstruct the targeted object. In case of medical imaging, an Ultrasound transducer (probe) is used both to focus and receive back the reflected ultrasound beam. Thus the field of view with such an ultrasound probe, is limited to a thin plane as shown in (Fig. 2.4).

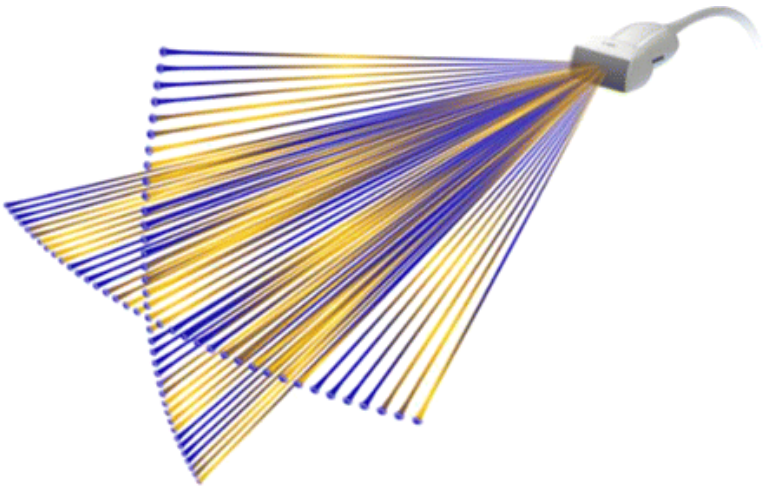

FIGURE 2.4: Vertical and horizontal imaging plane as seen from the ultrasound probe

The thickness of the plane depends on the thickness of the ultrasound probe. There are various available transducers with different bandwidth frequencies that defines the quality of the imaging. In our experiments, *Siemens Acuson S2000, (Siemens Healthcare, Mountain View, USA)* ultrasound system with a *18L6HD* probe is used for ultrasound imaging. The probe has a maximum bandwidth frequency of 18 MHz with a high quality HD reconstruction. Also the probe has a thickness of 4 mm which makes the ultrasound

plane thickness to also be 4 mm. The 4 mm thickness of the ultrasound plane would be sufficient enough to image both the gripper and the bead. The ultrasound system also has a frame rate of 60 fps. The gain of the signal is adjusted properly to obtain the clearest possible rendering.

Chapter 3

Tracking and Control of Soft, Self-folding, Hydrogel Grippers Using Ultrasound Images

Tracking and Control of Soft, Self-folding, Hydrogel Grippers Using Ultrasound Images

Krishna Kumar T. Chandrasekar, Stefeno Scheggi, Gert van de Steeg and Sarthak Misra

***Abstract*— For small scale agents, it is essential to possess untethered control in order to use them in hard to reach environments. This is now made possible by the advances in robotics and material science. Soft, self-folding, miniaturized hydrogel grippers have been developed that has the ability to perform several different pick and place tasks. In this paper, we exploit this feature of the hydrogel gripper for its potential use in bio-medical applications. Previous works on control of miniaturized grippers employed cameras equipped with microscopic lenses as feedback modality. However, the use of cameras might not be suitable for localizing miniaturized agents that navigate within the human body. We use the most common clinical imaging modality-ultrasound for knowing the position of the gripper. Accurate control has been performed by altering the magnetic field gradient and temperature of the workspace, thereby allowing us to control the position and grasping ability of the soft, self-folding magnetic grippers. The gripper was evaluated on different scenarios and motion profiles and it was found to achieve maximum accuracy with an average error of 0.42±0.12 mm without the payload. The micro sized payloads could be picked and moved with an average tracking error of 0.36±0.05 mm. The positioning accuracy achieved using our ultrasound based control system, proves the ability to control the miniaturized grippers in situations where digital camera feedback cannot be provided.**

I. INTRODUCTION

The fabrication and production of miniaturized grippers has now reached an all new level mainly due to the advances in material sciences. There has been experimental evaluations that prove these grippers could be used to pick-and-place small objects. Such agents with gripping abilities are advantageous in achieving complex tasks like precise micro-assembly, minimally invasive surgery, genetics, and cell manipulation [2]-[5]. Their tiny size are also compatible with the major vascular conduits, such that they can be used to safely grasp, manipulate and transport biological material [6],[7]. Recently, grippers have been demonstrated to autonomously pick-and-place biological material in a dynamic environment by the combination of tracking and closed-loop control [8],[9]. These works used images acquired by a camera. However, for these grippers to be used in clinical conditions, it is essential to design wireless magnetic based control, that could be controlled using clinically viable imaging modality.

Magnetic Resonance Imaging (MRI) has been used in the previous researches to detect and control magnetic drug carriers, nano-robots, and magnetotactic bacteria [10],[11]. However, a major drawback in using the MRI based tracking and actuation is the possibility of a delay being induced due to communications between the various modules of the interventional platform. It is highly essential for the tracking and realization of control to be in real time and such a time delay, could cause instability in the closed loop control system. On the other hand, Ultrasound (US) is one of the few cost efficient imaging modalities that has been used in the healthcare diagnostic industry for a long time, that could be used as an effective replacement for the camera. Factors like safe, positive effects to human health, adequate resolution and high frame rates, makes US a favorable choice [12]. US in the form of a high frequency ultrasound scanner had been used in the evaluation of of the motion of super paramagnetic iron oxide nanoparticles [13],[14]. Quadrature detection and phase gating at the frequency of interest formed the core algorithm behind it which provided the necessary feedback to control the motion of nanoparticles using US feedback. In [15] the author reports the results on closed-loop position control of paramagnetic microparticles under US guidance. Finally, Sanchez *et al.* tracked and controlled self-propelled, fast-moving microrobots using ultrasound feedback [16].

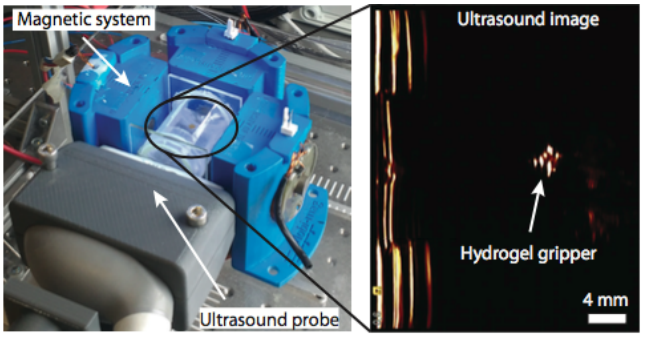

Fig. 1. The miniaturized gripper is placed in transparent reservoir, that is placed at the center of magnetic system. The magnetic system consists of three coils on a fixed frame, an Ultrasound transducer 18L6HD on the fourth direction and a peltier element on the bottom of the reservoir. The tracking and control of the grippers are performed on the image frames obtained from the ultrasound system (Siemens ACUSON S2000, Siemens Healthcare, Mountain View, USA)

In this work, the performance of soft, miniaturized hydrogel grippers that can be precisely localized and positioned in two-dimensional space using closed-loop ultrasound guided motion control, is demonstrated and analyzed. The US device is integrated to our magnetic based manipulation system for the purpose of feedback (Fig. 1) and the position of the grippers is determined from the obtained US images. Through the synergy of magnetic and

temperature control, the ability of the grippers to perform pick-and-move of micro-sized objects is demonstrated. Finally, the grippers are moved towards the reference position using a Proportional-Integral-Derivative (PID) magnetic-based control scheme.

The following chapters would explain the miniaturized gripper, its features and properties, followed by the experimental design, set up and finally walk through the experiments and their results.

II. Microgrippers

The small scale untethered robots has been proven to be used in a broad variety of applications, such as manipulation, assembly and micro-actuation [17]-[19]. However, these traditional, small robots are often passive with no shape-changing capabilities. This limits the robots in performing complex challenging tasks. On the other hand, agents with the ability to grip, provide significant advantages in achieving complex tasks. Precise micro-assembly, minimally invasive surgery, genetics, cell manipulation and mechanical characterization are few of the application that has been made possible by the use of small scale micro grippers [20]-[23]. For instance, Gultepe *et al.* demonstrated the feasibility of an *in vivo* biopsy of the porcine bile duct using thermally-responsive grippers [24]. Ichikawa *et al.* demonstrated the enucleation of bovine oocytes using untethered millimeter-scale grippers [22].

The studies mentioned above reveals and substantiates the idea of utilizing the small size of the miniaturized grippers in order to perform those tasks that would not have been possible through normal methods. But for the grippers to be used in medical applications, the following challenges are to be conquered. (1) The untethered operation has to be achieved in a much more smaller scale; (2) Accurate control of motion along with grabbing of the grippers has to be realized; (3) The grippers have to reliably manipulate micro-sized objects; (4) The grippers are to be made of biocompatible materials that can operate inside the persons body without posing any risk.

Size reduction and untethered actuation are critical to enable maneuverability of small-scale grippers in hard-to-reach environments. Conventional robotic approaches with electrical motors and actuators do not allow for significant miniaturization of the electronic components and on-board batteries. Hence, the use of wirelessly powered self-folding robots have drawn interest and shown promising results [25]-[31]. A family of prominent self-folding structures are composed of hydrogels that have several attractive properties of relevance to untethered small robots. Many grippers can be constructed with bio-compatible and even bio-degradable polymer chains or cross-linkers making them attractive for biomedical applications. They can function in aqueous media of relevance to biology and medicine. Their soft and squishy nature allows them to mimic the touch and feel of biological and even human appendages. Finally, they can be photopatterned into definite shapes so that they can change their shape on swelling and shrinkage [32].

A. Contribution

Our approach is validated using three different experiments. In the first one, the ability of the micro grippers to be localized and positioned in two-dimensional space using closed loop control is demonstrated. In the second scenario, obstacle free paths for the grippers are generated by adapting Linear Quadratic Gaussian Motion Planner (LQG-MP), by considering motion and sensing uncertainties. By using LQG-MP, we demonstrate that motion errors of the gripper can be taken into account during the planning phase, and proper obstacle-free paths can be computed in order to avoid collisions with the environment, e.g., sensitive organs or tissues. Finally with a synchronous magnetic and temperature control, we demonstrate the picking and moving of minute objects, which is tracked and controlled using Ultrasound images. To the best of author's knowledge, the reported results for the closed loop control of soft flexible micro grippers using US images to perform manipulation tasks, is the first of its kind.

The paper is organized as follows: Section III presents the electromagnetic system. Section IV-A describes the model and control techniques used in the experimental set up. Section IV- B discusses the image segmentation and tracking algorithms used. Section V presents and discusses the experimental results. Finally, Section VI concludes and provides directions for future work.

III. Modeling of Ultrasound based Control System

A. Magnetic and Thermal Systems

Our magnetic system consists of three electromagnets and an ultrasound probe, orthogonally placed surrounding the specially made container as shown in (Fig. 1). The Peltier element is attached bottom of the container as shown in (Fig. 1) [34]. The electromagnets are controlled using a proportional-integral-derivative (PID) controller [25][1]. Each electromagnet is powered by an Elmo Whistle 1/60 servo controller (Elmo Motion Control, Petach- Tikva, Israel). The system can generate magnetic fields with maximum magnitude of 15 mT with 60 mT/m gradients [1]. These magnetic fields are safe in clinical applications, where fields of up to 1.5 T are used daily in magnetic resonance imaging. The gripper can be successfully operated in three directions due to the presence of ultrasound probe in place of the fourth electromagnet. The motion control experiments with this system are deemed acceptable for the following reason: If the entire magnetic system could be expanded and recreated on a larger scale it would eventually provide much more space to accommodate both the electromagnet (coil) and the ultrasound probe. By this way, we would recreate a

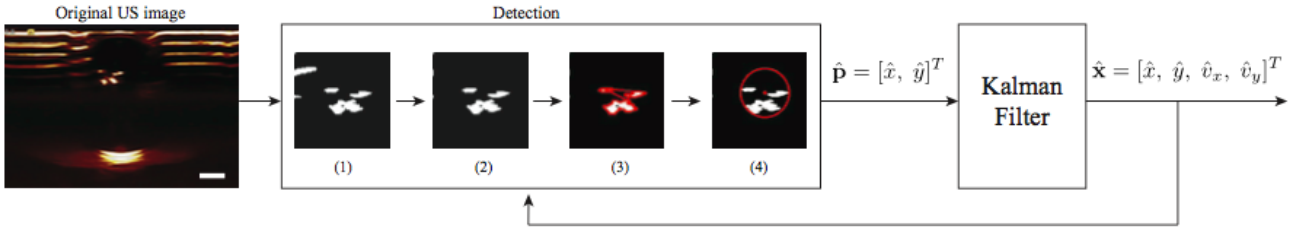

Fig. 2. Flowchart depicting the tracking process: From left to right, a B-mode image is obtained from the US machine. In the detection phase, only the Red channel of the Image is considered. (1) For proper detection of the gripper, a threshold is employed to the image. (2)Small blobs or blobs that are too far from the previous position of the gripper are removed, while merging the remaining adjacent blobs for further consideration. (3) The contours of the segments are computed. (4) A circle fitting is applied on the contour of the segmented area in order to detect the pose p = $[\hat{x},\ \hat{y}]^T$ of the gripper. Finally, state x of the gripper is estimated using a Kalman Filter, where $\hat{v}_x$, $\hat{v}_y$ represent the estimated velocities of the agent. Previously estimated state of the gripper is used in the current frame to speed up the detection procedure. The scale bar is 4 mm.

magnetic control system as demonstrated in [1], that would also work with ultrasound feedback.

The Peltier element is used for the purpose of temperature regulation of the water in which the grippers float. The element is attached to the bottom of the container using a conductive paste in such way that the temperature of the container could be maintained by the process of conduction. This setup of the peltier element could heat the water at an average rate of 10 °C/min [1].

B. Modeling and Control

The motion of the grippers are controlled by the use of magnetic based wireless control technique. This is entirely based on our currents that are used to control the electro-magnets into producing the right amount of electromagnetic forces to be exerted on grippers based on the function,

$$\mathbf{F(P)} = (\mathbf{m_{mg}}.\bigtriangledown)\mathbf{B(P)} = \wedge(\mathbf{m_{mg}}, \mathbf{P})\mathbf{I} \qquad (1)$$

where **F(P)** are the forces exerted on the grippers by the electromagnets, $\mathbf{B(P)} \in \mathbb{R}^{\mathbf{3\times1}}$ and $\mathbf{I} \in \mathbb{R}^{\mathbf{6\times1}}$ are the magnetic field produced by the electromagnets and their currents respectively and $\wedge(\mathbf{m_{mg}}, \mathbf{P}) \in \mathbb{R}^{\mathbf{3\times6}}$is the activation matrix, which converts the incoming currents into magnetic forces [39]. The magnetic forces are then managed and balanced accordingly using a two-input, three-output Multi-Input Multi-Output (MIMO) PID controller. The x and y co-ordinates of the gripper are fed as the two inputs to the controller. The output **F** is subsequently mapped into I using the pseudo-inverse of $\wedge(\mathbf{m_{mg}}, \mathbf{P})$ [15][1].

The knowledge of **B(P)** and $\mathbf{m_{mg}}$ is essential for computing the force-current map ($\wedge$). The **B(P)** of our setup has been evaluated in previous studies, using a finite elements model analysis, and successively verified using a calibrated three-axis Hall magnetometer [25]. The value of $\mathbf{m_{mg}}$ is estimated as explained Chapter II-B using the *U-Turn* experiments whereas the tracking procedure to obtain P is presented in Sec. IV [1].

IV. Tracking of Hydrogel Grippers

The entire motion control experiment depends mainly on the tracking accuracy of the tracker and the time taken by the algorithm to process each frame. The following section, describes the tracking algorithm used to estimate the position of the gripper.

Algorithm 1 Tracker algorithm

```
function Tracker(input, output, center, T)
    frame ← GetInputFrame
    for t = 1 to T do
        Crop frame to just the information area;
        Split frame Into RGB;
        Perform BINARY thresholding on R channel;
        Calculate Initial Center using Blob detection and
    Centroid method
        Using a Kalman Filter estimate center;
        Display the image back in the RGB channel.
        output ← frame
    Display the center with the frame & save it
```

Let $\mathrm{p} = [\mathbf{x}, \mathbf{y}]^{\mathbf{T}} \in \mathbb{R}^{\mathbf{2\times1}}$ be the position of a gripper in 2D space and $\mathrm{v} = [\mathbf{v_x}, \mathbf{v_y}]^{\mathbf{T}} \in \mathbb{R}^{\mathbf{2\times1}}$ its velocity. The state of the gripper is defined as $\mathrm{x} = [\mathbf{p}, \mathbf{v}] \in \mathbb{R}^{\mathbf{4\times1}}$. Let the miniaturized gripper be considered as a second order system controlled by applying suitable force inputs. The state $\hat{\mathbf{x}}$ of the gripper is estimated during run time by the tracking algorithm. (see Fig. 3). Initially the position $\hat{\mathbf{p}} = [\hat{\mathbf{x}}, \hat{\mathbf{y}}]^T$ of the gripper is estimated. In the first step, The RGB image is split into the separate R, G, B channels and only the R channel is considered by the algorithm. Then, binary thresholding is applied to the Red channel. Following it, the connected components concept is applied, wherein small blobs or blobs that are too far from the previous position of the gripper are removed, while merging the remaining adjacent blobs for further consideration. Finally, the contours of the remaining blobs are computed and the centroid of this contour is found out. The estimated position of the gripper $\hat{\mathbf{p}}$ corresponds to the center coordinates of the centroid estimated.

A standard Kalman filter [42] is implemented to consider the second order model of the gripper and control-inputs for estimating the state $\hat{\mathbf{x}}$ from the position estimates $\hat{\mathbf{p}}$. Assuming a constant sampling time Δt of the system, the

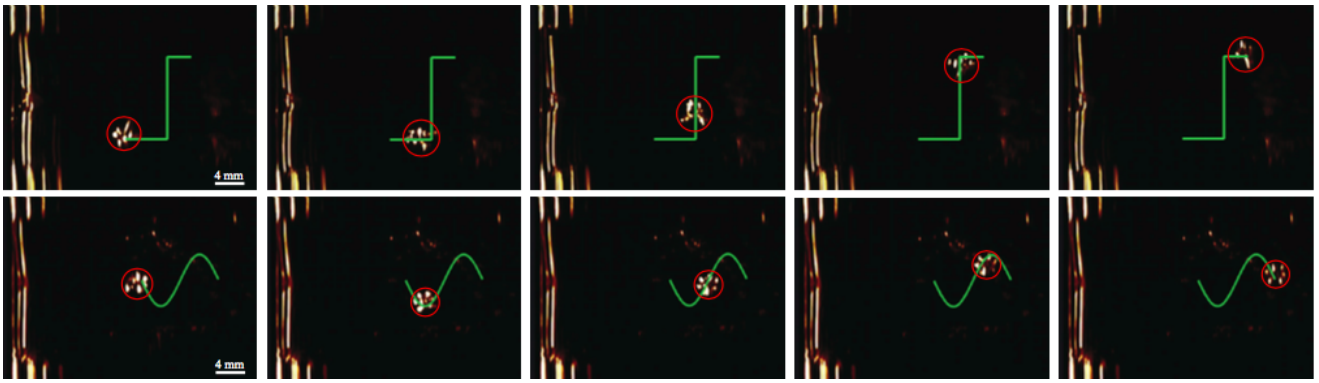

Fig. 3. Magnetic-based closed-loop motion control of an hydrogel gripper using ultrasound feedback. The gripper moves along the green path under the influence of the magnetic field gradients generated using a Proportional-Integral-Derivative controller coupled with the force-current map (2). The diameter of the gripper is approximately 4 mm. Top: step path. Bottom: sinusoidal path. Please refer to the accompanying video that demonstrates the path following control of a soft gripper using ultrasound feedback.

Kalman filter provides an estimation of the current state $\hat{\mathbf{x}}$ as well as a one-step ahead prediction of $\hat{\mathbf{x}}$. The zero mean multivariate Gaussian distributions N(0,**Q**) and N (0, **R**) are used to estimate the process and measurement noises, respectively, where $\mathbf{Q} \in \mathbb{R}^{4\times4}$ and $\mathbf{R} \in \mathbb{R}^{2\times2}$ are the empirically determined covariance matrices.

Temporal continuity is exploited to track the grippers in a sequence of frames, to speed up the detection procedure. Given the estimated state $\hat{\mathbf{x}}$ of the tracked gripper from the previous frame, only a preset window of pixels around the estimated center are considered, discarding the rest. The proposed tracker runs at an average frame rate of 100 frame per second on a PC that has an Intel Xeon CPU 3.2 GHz processor and 8 GB of RAM.

A series of image sequences were used to test and evaluate this method. Three video sequences were considered, which report the common motion of the miniaturized grippers during manipulation and transportation tasks. In particular, the first two sequences motions of the miniaturized gripper are reported, while in the last sequence the folding of the grippers for the manipulation tasks are captured (see Fig. 4). The video sequences have 1298, 927, and 2229 frames, respectively. Every frame of the three sequences is manually labeled by marking the approximate center position of the gripper in each frame, in order to generate ground truth data for the evaluation of the tracker. This is the most appropriate approach followed by most relevant literatures, since ground truth data for such motion actions are hard to obtain. The evaluation shows a tracking error of 0.51 $\pm$ 0.33 mm, 0.49 $\pm$ 0.26 mm, and 0.26 $\pm$ 0.13 mm, for the three sequences, respectively. The tracking errors correspond to 12.7$\pm$8.25 %, 12.25$\pm$6.5 %, and 6.5$\pm$3.25 % of the body length of the miniaturized gripper.

V. Experimental Validation

In this section we assess the capabilities of the grippers. We report three different experiments in order to show the possibility for the soft grippers to: (1) follow a predefined path, (2) autonomously move in a cluttered environment, and (3) firmly grasp an object and transport it to a target area.

A. Motion Control

In this experiment, we evaluate the performance of control and accuracy of tracking the motion for point-to-point motion and few other pre-defined motion profiles, namely the Step motion and Sine motions. The experiments were repeated for 10 times each over grippers chosen from 5 different batches. These experiments were performed without any non-magnetic payload. The mean and standard deviation of the motion of the gripper are plotted and shown in figure [Fig. 6]. For the plots the ultrasound probe is placed on to the left side of the plot and the gripper is made to trace the path from left to right.

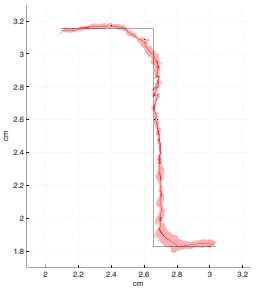

Fig. 4. (a)

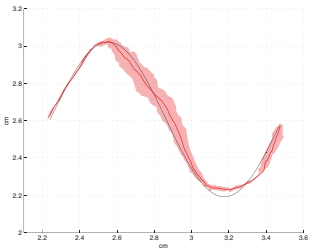

Fig. 5. (b)

Fig. 6. Sine and step plots that has the mean and Standard deviation of 10 trials. The Black line denotes the reference path, the red line denotes the average path traced by the gripper and the red smudge denotes the Standard deviation of the gripper. Fig 5 shows the Step plot. Fig 6 denotes the Sine plot.

The gripper has a average positioning error of 0.3 $\pm$0.03 mm and 0.48$\pm$0.1 mm with an average velocity of 0.33$\pm$0.1 mm/s and 0.41$\pm$0.14 mm/s for the step and the sine trajectories respectively. *Kindly refer to the video evidence for better understanding.* With respect to the body size of the gripper,

we have calculated that the average error was 7.5±0.75 % and 10 ± 2.5 % respectively. These errors occur partly due to the lack of coil 4 and partly due to partial or noisy measurements of the agents state. Since the pull is only in 3 directions, a lowest acceptable error threshold is found using various trails to filter and control the gripper efficiently. The threshold was calculated from a series of motion experiments and this acceptable threshold is found out to be 2 mm, below which the gripper overshoots and stops moving and above which the error tends to be very high.

B. Motion planning with motion uncertainty and imperfect state information

The next important feature required by the miniaturized agents to successfully complete a desired task, is its ability to move autonomously towards the target by choosing an obstacle free path that is also short and safe. Results presented in Sect. V-A show that motion uncertainty, e.g. due to un-modeled external influences on the motion of the agent, and imperfect state information due to partial or noisy measurements of the agents state, generate positioning errors. The amount of motion and sensing uncertainty depend on : (1.) The particular motion executed by the gripper; and (2.) The state of the agent. Thus different trajectories of the agent would have different uncertainties associated with them. However, since safety and accuracy are of critical importance for many medical tasks, these uncertainties would have a significant impact on best path chosen for the task at hand. Thus path planning algorithms were developed in order to successfully perform the task minimizing these uncertainties. The algorithm that is used to generate a set of paths by utilizing *Rapidly exploring Random Tree (RRT)* is shown below.

Algorithm 2 Planner algorithm

function RRT($x_{init}, T, \delta t, X_{goal}$)
  $\tau.add(x_{init})$
  for $t = 1toT$ **do**
    $x_{rand} \leftarrow RandomState()$;
    $x_{near} \leftarrow NearestNeighbour(x_{rand,\tau})$;
    $u_t \leftarrow SelectInput(x_{near}, x_{rand})$;
    $x_{new} \leftarrow NewState(u_t, x_{near}, \delta t)$;
    $\tau.add(x_{new})$;
  if $x_T \in X_{goal}$ **then**
    return $reached$
  else
    return $failed$
  return τ

Following the generation of paths, the *a-priori* variances is computed and the most optimal path is estimated. This evaluation is based on the Linear Quadratic Gaussian Motion Planning (LQG-MP) algorithms. By this, various possible scenarios were simulated and evaluated. These were experimentally verified with the miniaturized gripper. The gripper was tested over 10 iterations for a specifically chosen scenario. The experimental example with estimated paths is shown in (Fig. 7). The algorithm runs for 3 seconds and generates 30 successful motion plans. The final plan was selected using the LQG-MP approach by maximizing the distance from the obstacles (minimizes the chances of collision). The gripper was demonstrated to reach the target location from an initial location using the selected final plan *Please look up for the added video evidence for better understanding.*

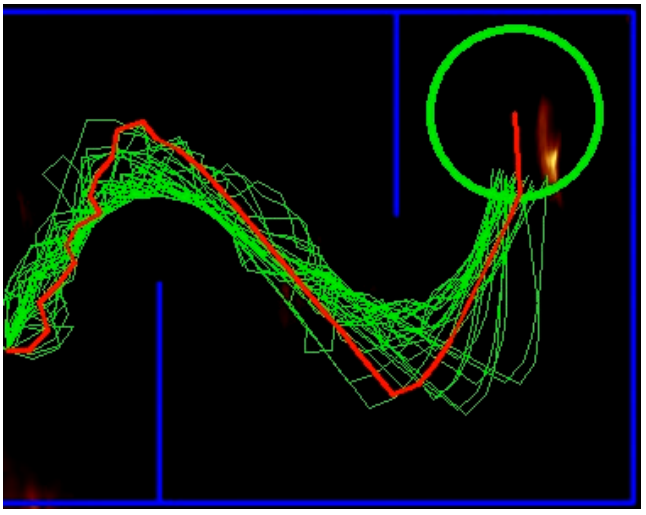

Fig. 7. Path planner showing the estimated path. The green circle denotes the target location, The blue lines represent the boundary and static obstacles, the green lines are all the possible paths estimated and the red path denotes the most optimum chosen path.

C. Pick and Move

In this section, the ability of the grippers to perform pick and move tasks (transportation) is highlighted. The gripper is positioned above a 500 μm spherical plastic bead, which serves as the object to be picked and moved. Now the distance between the bead and position of the gripper above it has to be exactly 3 mm. The ultrasound has a very narrow field of vision, that extends to a plane of thickness of 4 mm and thus the distance between the gripper and the bead should not be more than 3 mm to successfully image both the bead and the gripper using ultrasound. The distance between the gripper and bead below should not be less than 3 mm. This is due to the fact that the a fully open gripper has a diameter of 4 mm, which makes it difficult for the gripper to successfully grab the bead.

When the experiment is started, the gripper is controlled, moved from the initial position and positioned over the bead. Once the gripper is positioned above the bead, the temperature is increased to 30° C. This forces the gripper to close and the placement of the gripper, allows the bead to be picked by it. Therefore the micro-sized payload is captured within the gripper, which makes it possible to carry and transport the bead to the desired location. An *L* trajectory path is planned for the gripper to moved to the desired location. The experiment is repeated for ten

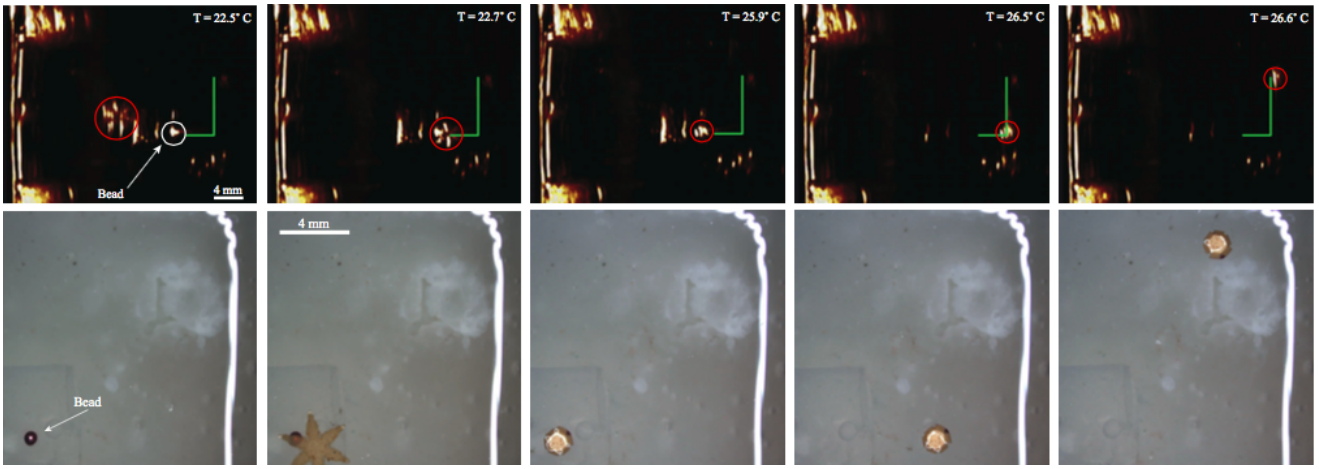

Fig. 8. Video snapshots of the gripper during manipulation and transportation of a 0.5 mm bead. The gripper is moved from the initial position towards the bead. Once the bead is reached, the temperature is increased until the system classifies the gripper as closed. The gripper is then guided to the target area through a predefined trajectory. Temperatures (T) are shown on the top-right corner of each snapshot. Top: video sequence acquired using an ultrasound probe. Bottom: in order to facilitate the readers understanding of this experiment, we provide the video sequence acquired with a microscopic camera. Please note that the magnetic controller uses only the feedback provided by the ultrasound probe. Please refer to the accompanying video for this experiment.

times and the average positioning error was 0.36±0.05 mm. The micro-sized payload was successfully transported and moved in the specified path for a distance of 14.5 mm with an average velocity of 0.39±0.06 mm/s. The video accompanying this document explains the process much more elaborately.

VI. Discussion and Conclusion

In this paper, we make use of the characterized soft, self-folding grippers and analyze their capabilities and performance using medical imaging modality, ultrasound. The gripper could be localized and could follow trajectories (sine and step) with a maximum average positioning error of 0.48 with a variance of 0.1 mm. The grippers were being autonomously maneuvered through simulated environments with the presence of static obstacles. The gripper was found to assess the environment, simulate upto 30 different paths in 3 seconds and move along the most optimum selected path to reach the target location. Finally the pick and move experiments were completed with an average error of 0.36±0.05 mm with an average velocity of 0.39±0.06 mm/s. For our study, sine and step trajectories are the best possible trajectories that could be demonstrated in a magnetic system that could operate in three directions. With the obtained results it is possible prove that the grippers could be controlled and positioned in two dimensional space to perform manipulative tasks successfully. Also, if this magnetic system is expanded and recreated on a larger scale, there would be enough space to accommodate both the electromagnet and the ultrasound probe, thereby recreating a magnetic control system as demonstrated in [1]. By this way, it is possible to generalize the system for other scenarios. The most important factor is the built of the miniaturized gripper, that makes it possible to visualize, track and control them using ultrasound images. These experiments are also made possible by the following two most important advances in field of robotics and material science; (1) The development in the production of soft, reversible micro grippers that does not require external sources of energy for their activation owing to their shape changing by swelling property; (2) The possibility to control with precision the local temperature and magnetic field using closed loop operations.

As a part of future work, the control of the grippers will be studied to implement three dimensional control. Also more advanced scenarios will be developed and tested which would eventually be used pick and move experiments. Further more, cooling system will be designed and implemented for pick and place experiments. More intricate path planning methodologies for a system with both static and dynamic obstacles, will be developed for more realistic scenarios. This presented system will be extended to clinical experimentation for clinically relevant applications.

References

[1] F. Ongaro et al., "Control of untethered soft grippers for pick-and-place tasks," 2016 6th IEEE International Conference on Biomedical Robotics and Biomechatronics (BioRob), Singapore, 2016, pp. 299-304.

[2] N. Dechev, W. L. Cleghorn, and J. K. Mills. Microassembly of 3-d microstructures using a compliant, passive microgripper. J. of Microelectromechanical Systems, 13(2):176189, 2004.

[3] T. Yoneyama, T. Watanabe, H. Kagawa, J. Hamada, Y. Hayashi, and M. Nakada. Force detecting gripper and flexible micro manipulator for neurosurgery. In Proc. IEEE Int. Conf. on Engineering in Medicine and Biology Society, pages 66956699, 2011.

[4] A. Ichikawa, S. Sakuma, F. Arai, and S. Akagi. Untethered micro-robot with gripping mechanism for on-chip cell surgery utilizing outer magnetic force. In Proc. IEEE Int. Conf. on Robotics and Automation, pages 37953800, 2014.

[5] M. M. S. Mousavi, G. De Pasquale, A. Soma', and E. Brusa. A novel su-8 microgripper with external actuator for biological cells manipulation. In Proc. Symp. on Design, Test, Integration & Packaging of MEMS and MOEMS, pages 356361, 2011.

[6] F. Hansen, P. Mangell, B. Sonesson, and T. Lanne. Diameter and compliance in the human common carotid arteryvariations with age and sex. Ultrasound in Medicine & Biology, 21(1):19, 1995.

[7] F. Beyeler, A. Neild, S. Oberti, D. J. Bell, Y. Sun, J. Dual, and B. J. Nelson. Monolithically fabricated microgripper with integrated force sensor for manipulating microobjects and biological cells aligned in an ultrasonic field. J. of Microelectromechanical Systems, 16(1):715, 2007.

[8] F.Ongaro,C.Pacchierotti,C.Yoon,D.Prattichizzo,D.H.Gracias,and S. Misra. Evaluation of electromagnetic system with haptic feedback for control of untethered, soft grippers affected by disturbances. In Proc. IEEE RAS/EMBS Int. Conf. on Biomedical Robotics and Biomechatronics, pages 908913, 2016.

[9] S. Scheggi, C. Yoon, D. H. Gracias, and S. Misra. Model-based tracking of miniaturized grippers using particle swarm optimization. In Proc. IEEE/RSJ Int. Conf. on Intelligent Robotic Systems, In Press, 2016.

[10] S. Martel, O. Felfoul, J.-B. Mathieu, A. Chanu, S. Tamaz, M. Mohammadi, M. Mankiewicz, and N. Tabatabaei. MRI-based medical nanorobotic platform for the control of magnetic nanoparticles and flagellated bacteria for target interventions in human capillaries. Int. J. of Robotic Research, 28(9):11691182, 2009.

[11] J.-B. Mathieu and S. Martel. Steering of aggregating magnetic microparticles using propulsion gradients coils in an MRI scanner. Magnetic Resonance in Medicine, 63(5):13361345, 2010.

[12] B. J. Nelson, I. K. Kaliakatsos, and J. J. Abbott. Microrobots for minimally invasive medicine. Annual Review of Biomedical Engineering, 12:5585, 2010.

[13] M. Evertsson, M. Cinthio, S. Fredriksson, F. Olsson, H. W. Persson, and T. Jansson. Frequency-and phase-sensitive magnetomotive ultrasound imaging of superparamagnetic iron oxide nanoparticles. IEEE Trans. on Ultrasonics, Ferroelectrics, and Frequency Control, 60(3):481491, 2013.

[14] J Weizenecker, B Gleich, J Rahmer, H Dahnke, and J Borgert. Three-dimensional real-time in vivo magnetic particle imaging. Physics in Medicine and Biology, 54(5):L1, 2009.

[15] I. S. M. Khalil, L. Abelmann, and S. Misra, "Magnetic-based motion control of paramagnetic microparticles with disturbance compensation," IEEE Transactions on Magnetics, vol. 50, no. 10, pp. 110, 2014.

[16] A. Sanchez, V. Magdanz, O. G. Schmidt, and S. Misra, "Magnetic control of self-propelled microjets under ultrasound image guidance," in Proceedings of the IEEE RAS & EMBS International Conference on Biomedical Robotics and Biomechatronics, pp. 169174, Sao Paulo, Brazil, August 2014.

[17] S. Martel and M. Mohammad, "Using a swarm of self-propelled natural microrobots in the form of flagellated bacteria to perform complex micro-assembly tasks," in Proceedings of the IEEE International Conference on Robotics and Automation (ICRA), pp. 500505, Alaska, USA, May 2010.

[18] S.Tottori,L.Zhang,F.Qiu,K.K.Krawczyk,A.Franco-Obrego n,and B. J. Nelson, "Magnetic helical micromachines: fabrication, controlled swimming, and cargo transport," Advanced materials, vol. 24, no. 6, pp. 811816, 2012.

[19] M.Sitti,H.Ceylan,W.Hu,J.Giltinan,M.Turan,S.Yim,andE.Diller, "Biomedical applications of untethered mobile milli/microrobots," Proceedings of the IEEE, vol. 103, no. 2, pp. 205224, 2015.

[20] J. S. Randhawa, T. G. Leong, N. Bassik, B. R. Benson, M. T. Jochmans, and D. H. Gracias, "Pick-and-place using chemically actuated microgrippers," Journal of the American Chemical Society, vol. 130, no. 51, pp. 17 23817 239, 2008.

[21] E. Diller and M. Sitti, "Three-dimensional programmable assembly by untethered magnetic robotic micro-grippers," Advanced Functional Materials, vol. 24, no. 28, pp. 43974404, 2014.

[22] A. Ichikawa, S. Sakuma, F. Arai., and S. Akagi, "Untethered microrobot with gripping mechanism for on-chip cell surgery utilizing outer magnetic force," in Proceedings of the IEEE International Conference on Robotics and Automation (ICRA), pp. 37953800, Hong Kong, China, May 2014.

[23] K. Malachowski, M. Jamal, Q. Jin, B. Polat, C. J. Morris, and D. H. Gracias, "Self-folding single cell grippers," Nano Letters, vol. 14, no. 7, pp. 41644170, 2014.

[24] E. Gultepe, J. S. Randhawa, S. Kadam, S. Yamanaka, F. M. Selaru, E. J. Shin, A. N. Kalloo, and D. H. Gracias, "Biopsy with thermally-responsive untethered microtools," Advanced Materials, vol. 25, no. 4, pp. 514519, 2012.

[25] J. S. Randhawa, K. E. Laflin, N. Seelam, and D. H. Gracias, "Microchemomechanical systems," Advanced Functional Materials, vol. 21, no. 13, pp. 23952410, 2011.

[26] K. Malachowski, J. Breger, H. R. Kwag, M. O. Wang, J. P. Fisher, F. M. Selaru, and D. H. Gracias, "Stimuli-responsive theragrippers for chemomechanical controlled release," Angewandte Chemie, vol. 126, no. 31, pp. 81838187, 2014.

[27] S. Fusco, M. S. Sakar, S. Kennedy, C. Peters, R. Bottani, F. Starsich, A. Mao, G. A. Sotiriou, S. Pane , S. E. Pratsinis et al., "An integrated microrobotic platform for on-demand, targeted therapeutic interventions," Advanced Materials, vol. 26, no. 6, pp. 952957, 2014.

[28] S. Fusco, M. S. Sakar, S. Kennedy, C. Peters, S. Pane, D. Mooney, and B. J. Nelson, "Self-folding mobile microrobots for biomedical applications," in Proceedings of the IEEE International Conference on Robotics and Automation (ICRA), pp. 37773782, Hong Kong, China, 2014.

[29] J. C. Kuo, H. W. Huang, S. W. Tung, and Y. J. Yang, "A hydrogel-based intravascular microgripper manipulated using magnetic fields," Sensors and Actuators A: Physical, vol. 211, pp. 121130, 2014.

[30] S. Miyashita, S. Guitron, M. Ludersdorfer, C. R. Sung, and D. Rus, "Untethered miniature origami robot that self-folds, walks, swims, and degrades," in Proceedings of the IEEE International Conference on Robotics and Automation (ICRA), pp. 14901496, Seattle, WA, USA, May 2015.

[31] H.Li,G.Go,S.Y.Ko,J.-O.Park,andS.Park,"Magneticactuatedph- responsive hydrogel-based soft micro-robot for targeted drug delivery," Smart Materials and Structures, vol. 25, no. 2, p. 027001, 2016.

[32] D. H. Gracias, "Stimuli responsive self-folding using thin polymer films," Current Opinion in Chemical Engineering, vol. 2, no. 1, pp. 112119, 2013.

[33] J. C. Breger, C. Yoon, R. Xiao, H. R. Kwag, M. O. Wang, J. P. Fisher, T. D. Nguyen, and D. H. Gracias, "Self-folding thermo-magnetically responsive soft microgrippers," ACS Applied Materials & Interfaces, vol. 7, no. 5, pp. 33983405, 2015.

[34] A. Sanchez, Y. M. Sadek, I. S. M. Khalil, and S. Misra, "Mobimag: A compact device for medical research using wireless control of magnetic microrobots," in Proceedings of the Design of Medical Devices Conference-Europe, pp. 100101, Delft, Netherlands, October 2014.

[35] G. F. Franklin, J. D. Powell, and A. Emami-Naeini, "Feedback control of dynamics systems," Addison-Wesley, Reading, MA, 1994.

[36] A. S. Bahaj, P. A. B. James, and F. D. Moeschler, "An alternative method for the estimation of the magnetic moment of non-spherical magnetotactic bacteria," IEEE Transactions on Magnetics, vol. 32, no. 5, pp. 51335135, 1996.

[37] Y.R.Chemla,H.L.Grossman,T.S.Lee,J.Clarke,M.Adamkiewicz, and B. B. Buchanan, "A new study of bacterial motion: supercon- ducting quantum interference device microscopy of magnetotactic bacteria," Biophysical Journal, vol. 76, no. 6, pp. 33233330, 1999.

[38] W. F. Brown, "Magnetostatic principles," in Ferromagnetism. North-Holland Amsterdam, 1962.

[39] I. S. M. Khalil and S. Misra, "Control characteristics of magnetotactic bacteria: Magnetospirillum Magnetotacticum strain MS-1 and Magnetospirillum Magneticum strain AMB-1," IEEE Transactions on Magnetics, vol. 50, no. 4, pp. 111, 2014.

[40] F. Van der Heijden, "Image based measurement systems: object recognition and parameter estimation." John Wiley & Sons Ltd, 1994.

[41] M. He, "The faber polynomials for m-fold symmetric domains," Journal of Computational and Applied Mathematics, vol. 54, no. 3, pp. 313324, 1994.

[42] P.R.Belanger, P.Dobrovolny, A.Helmy, and X.Zhang, "Estimation of angular velocity and acceleration from shaft-encoder measurements," The International Journal of Robotics Research, vol. 17, no. 11, pp. 12251233, 1998.

[43] G. B. Limentani, M. C. Ringo, F. Ye, M. L. Bergquist, and E. O. McSorley, "Beyond the t-test: statistical equivalence testing," Analytical Chemistry, vol. 77, no. 11, pp. 221226, 2005.

Chapter 4

Comparison of Histogram of Gradients and HAAR Cascade Classifier for Tracking Micro Agents using Ultrasound Images

Comparison of Histogram of Gradients And HAAR Cascade Classifier For Tracking Micro Agents Using Ultrasound Images

Krishna Kumar T. Chandrasekar, Stefeno Scheggi, Gert van de Steeg and Sarthak Misra

Abstract— **The usage of miniaturised agents in magnetic based drug delivery systems and clinical biopsies could be made affordable if it is possible to control them wirelessly based on the feedback obtained from the common clinical imaging techniques such as the ultrasound(US). But since the image from US does not have sharp edges, the most common detection techniques used in digital image processing has to to be modified and adapted in such a way, the control of the micro agent is made possible. In order to evaluate such clinically relevant scenarios, algorithms and features descriptors such HAAR and HOG were selected and compared for exploring the best possible features from the ultrasound images and eventually based on the results, a specialized tracker was formulated with aim of tracking the miniaturized gripper in real tissue type of environment. For this purpose, synthetic datasets were developed from real tissue samples and the tracker was trained and tested with those datasets. The proposed tracker had a tracking accuracy of 81%.**

I. INTRODUCTION

The fabrication and production of micro sized tiny grippers has now reached all new level basically due to the advances in material sciences. The previous experiments prove that these grippers could be used for pick and place objects relative to the size of the grippers. For these grippers to be used in clinical conditions, we have to come up with more cost efficient and proven ways to track and control the grippers. Ultrasound is one of the few cost efficient imaging modalities that has been used in the healthcare industry for years now, which could be an effective replacement for the camera. The basic principle of ultrasound imaging is very similar to that of a sonar where a concentrated beam of ultrasound waves is focussed on to the target direction and the reflected wave processed as the image. From the obtained image, based on the material and frequency of the ultrasound, the basic shape of the object could be obtained. Thus this imaging method could used to locate and control of gripper. Yet, taking it closer towards the clinical conditions has a few problems that are to be addressed that are listed as follows

- Gripper classification has to extremely precise and accurate,
- In clinical condition, there would be the real tissues imaged along with the gripper and the classifier has to effectively track the gripper in those complex conditions,
- The computation time per frame has to be as low as possible for better control.,

Most of the detecting methods comprise of two basic steps: Hypothesis Generation (HG) and Hypothesis Verification (HV) (Sun *et al.*, 2006). HG approaches are very simple low level algorithms that are used to locate potential object locations and can be classified in three categories:

- - knowledge-based: symmetry (Bensrhair et al., 2001), colour (Xiong and Debrunner, 2004; Guo et al., 2000), shadows (van Leeuwen and Groen, 2001), edges (Dellaert, 1997), corners (Bertozzi et al., 1997), texture (Bucher et al., 2003), etc.,
- - stereo-based: disparity map (Franke, 2000), inverse perspective mapping (Bertozzi and Broggi, 1997), etc,
- - stereo-based: disparity map (Franke, 2000), inverse perspective mapping (Bertozzi and Broggi, 1997), etc,

The HG step outputs the Region of Interest that is validated using the HV approaches. The HV approaches can be grouped in two categories: template-based and appearance-based.

- Template-based methods maps the relationship between a predefined pattern of the object class and the input image: horizontal and vertical edges (Srinivasa, 2002), regions, deformable patterns (Collado et al., 2004) and rigid patterns (Yang *et al.*, 2001).
- Appearance-based methods usually train the system with the knowledge of the classes The Object and Nonobject from a set of training images. Each training image is represented by a set of local or global descriptors (features) (Agarwal *et al.*, 2004). Following this, the classification algorithms would estimate the decision boundary between the two classes.

Object recognition and tracking is one of the prime researched topics pertaining to computer vision. Various techniques have been developed over the years that could effectively track different types of objects. Template based methods has always been of great help in object tracking. Deformable patterns (Collado et al., 2004) and rigid patterns (Yang *et al.*, 2001) are highly successful in many object identification approaches. However, in our case, we have a soft hexagonal shaped gripper that has the ability to change its orientation and shape according to its condition. Finding a pattern out of such a shape changing ultrasound imaged gripper is extremely time consuming. Thus template based methods would not be an efficient idea to be implemented in this scenario. On the other hand, appearance based methods, train the system with the knowledge of the classes, just once during the training phase. This makes it extremely efficient for utilizing them in real time tracking applications. In [14] is described a

novel method, where an carotid artery is detected using the grammar-guided genetic programming (GGGP). The GGGP combines simple image processing methods and chooses the best possible combination that results in highest detection precision. Another work for object detection is presented in [15]. In this work, animal heads were detected. The method was based on the Viola-Jones detector, which used Haar of Oriented Gradients (HOOG) as a weak classifier. HOOG is combination of Haar-like features and Histograms of Oriented Gradients (HOG) method [16]. Therefore it benets from both, for the shape recognition Haar-like features are used and for the texture recognition HOG method is used. [17] explained a trained Viola-Jones detector for the detection of rotated faces in image. Detected faces were shown with value of rotation in degrees.

The HAAR and HOG feature descriptors are widely used mainly on pedestrian and faces classification. The HAAR classifier, predominantly uses the features that could eventually classify based on the shape while the HoG descriptor would use the texture of the object for classification. For the input ultrasound image we study and compare the performance parameters of the two feature descriptors using the different testing datasets and thereby suggesting a micro agent tracker model.

The following section explains briefly the HAAR and HoG features. Section 3 demonstrates the Learning algorithms - AdaBoost used for the training of weak classifier. The paper concludes with a comparison of the descriptors based on its performance and our suggested tracking model.

II. Features

The common reasons why features are chosen instead of pixels values are that features can code high level object information (segments, texture, ...) while intensity pixel values based system operates slower than a feature based system. This section describes the features used to train the Adaboost cascade.

A. Haar filters

Papageorgiou *et al.* (Papageorgiou and Poggio, 1999) introduced the use of set of 2D wavelets and demonstrated the detection vehicles in static images. (Fig. 1) shows the basic Haar filters: two, three and four rectangle features, where the sum of the white pixels is subtracted from the sum of grey pixels in the rectangles. In the original paper, Papageorgiou had made use of only the two and three rectangle features due to the logical reason that these two features define most of the vehicles information and the diagonal feature would only be an extra information of the same definition conveyed by the other two features. In our case since the gripper is star shaped, the diagonal feature would also provide new information and we would these features as well.

Viola and Jones in 2001 (Viola and Jones, 2001) introduced the concept of Integral Image, an intermediate

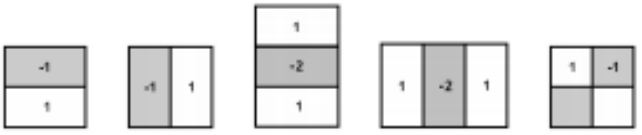

Fig. 1. 2-D HAAR wavelet sets

representation for the input image, which reduces the computation tremendously. As per the idea of Integral Image, the sum of the rectangular region in the image can be calculated with as low as four Integral Image references. In a similar way, the difference between two adjacent rectangles can be computed with only six references, eight in the case of the three-rectangle feature. The rectangular filters obtained from various scales of the image results in the formation of the Haar feature set. The important subtraction values are denoted by the lightness pixels (the result is always calculated in modulus).

The complete set of Haars features utilizing the three rectangular filters (see fig. 1) in a 90x90 pixel image at 2,4,8,16 scales is 11378. Every single feature j in the set could be defined as: fj = (xj ,yj ,sj ,rj), where rj is the rectangular filter type, sj the scale and (xj ,yj) are the position over the 32x32 image.

B. Histogram of Oriented Gradient

The Histogram of Gradients (HoG) can be defined as an yet another method that can be utilized to obtain a vector of visual descriptors by encoding the input image. The local descriptor makes use of the orientation and gradient magnitude around a key point location thereby constructing the resulting histograms. This method is based on Scale invariant Feature Transform (SIFT). The number of bins in the histogram quantizes the orientations (four orientations is sufficient). For every histogram bin, the magnitudes of similar orientations are grouped and added together.

Following the addition, in order to get the values between 0 and 1, the histogram values are normalized using overall total energy value of all orientations. For a two class problem, Gepperth (Gepperth et al., 2005) trained the first neural network classifier using the HoG features. The method used by the author was pretty simple wherein fixed number of regions called the Receptive Fields was defined by subdividing the ROI from which oriented histogram feature was obtained individually. The HoG feature set comprises of the histograms that calculated from this rectangular region defined in the original image. To get the gradient magnitude and orientation, Sobel filters is used for the evaluation of the gradient of the image.

There are three types of rectangle regions: r1 square l*l, r2 vertical rectangle l*2l, r3 horizontal rectangle 2l*l. Considering l : 2,4,8,16 scales, we have a total of 4678 features. A single histogram j in the set could be defined

as: hj = (xj ,yj ,sj ,rj), where rj is the rectangular filter type, sj the scale and (xj ,yj) are the position over the 90x90 image.

III. ADABOOST

With respect to the previous sections, we have seen that the Haar and HoG are vector representations of the image in the form of visual descriptors. The total number of features calculated is clearly more than total number of pixels in the image, which makes it computationally very intensive to use all the features to perform the classification. This is mainly because there are a lot of these features without quality information, thereby forcing alternative methods for better and faster classification. Some of the methods that are used to limit the number of features are statistics (Schneiderman and Kanade, 2000), PCA, genetic algorithms (Sun et al., 2004), etc.

Out of these, one form of ensemble learning that improves the performance of any algorithm is Boosting (Freund and Schapire, 1996). It finds precise hypothesis by combining several weak classifiers, which on average, have a moderate precision. The weak classifiers are then combined to create a strong classifier:

$$G = \begin{cases} \sum_{n=1}^{N} \alpha_n g_n \geq \frac{1}{2} \sum_{n=1}^{N} \alpha_n = T \\ 0 \quad \text{otherwise} \end{cases} \tag{1}$$

Where $\mathbf{G}$ and $\mathbf{g}$ are the strong and weak classifiers respectively and $\boldsymbol{\alpha}$ is a coefficient, weighing each feature result. $\mathbf{T}$ is the strong classifier threshold. There are different variants of boosting such as Discrete Adaboost (Viola and Jones, 2001), Real AdaBoost (Friedman et al., 2000), Gentle AdaBoost, etc. The procedures (pseudo-code) of any of this variants are widely developed in the literature. We need, however, to study the construction of the weak classifier for both cases: Haar and HoG features.

A. Haar Weak classifier

We define the weak classifier as a binary function g:

$$g \begin{cases} 1 & \text{if } p_j f_j < p_j \theta_j \\ 0 & \text{otherwise} \end{cases} \tag{2}$$

where $\boldsymbol{f_j}$is the feature value, $\boldsymbol{\theta_j}$ the feature threshold and $\boldsymbol{p_j}$ the threshold parity.

B. HoG Weak classifier

This time, instead of evaluating a feature value, we estimate the distance between an histogram $\mathbf{h_j}$ of the input image and a model histogram $\mathbf{m_j}$. The model is calculated like the mean histogram between all the training positive examples. For each histogram $\mathbf{h_j}$ of the feature set, we have the corresponding $\mathbf{m_j}$. A vehicle model is then constructed and AdaBoost will find the most representative $\mathbf{m_j}$ which best separate the vehicle class from the non-vehicle class. We define the weak classifier like a function g:

$$g \begin{cases} 1 & \text{if } d(h_j, m_j) < \theta_j \\ 0 & \text{otherwise} \end{cases} \tag{3}$$

where $\mathbf{d}(\mathbf{h_j}(\mathbf{x}), \mathbf{m_j})$ is the Bhattacharyya distance (Cha and Srihari, 2002) between the feature $\mathbf{h_j}$ and $\mathbf{m_j}$ and $\boldsymbol{\theta_j}$ is the distance feature threshold.

IV. TRAINING

A. Dataset

In order to obtain a detector that could successfully classify the miniaturized gripper, it is essential to have a specialized dataset, that could be used to train the detector. Thus Dataset plays a crucial role in the overall performance of the detector. Since, the dataset forms the backbone of training, it forms the core of the entire solution. To move closer towards real-time clinical conditions, a complex synthetic dataset was synthesized by super imposing the normal miniaturized gripper dataset with dataset from a human tissue.

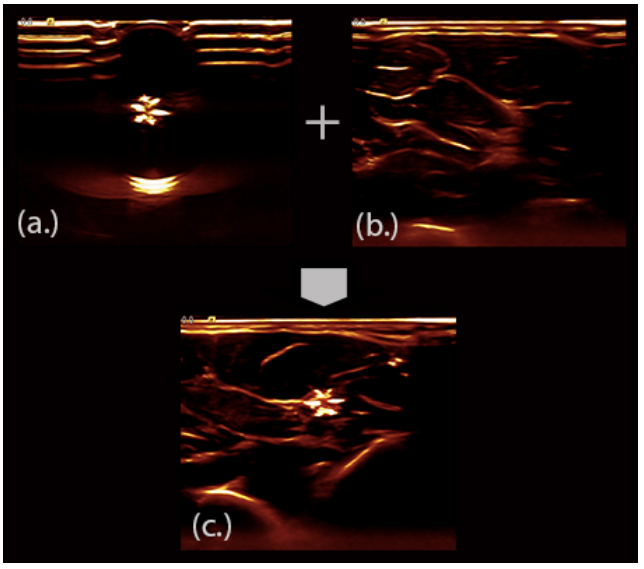

Fig. 2. This image explains how a synthetic dataset, that mimics the miniaturized gripper to be operating in a real tissue medium is created. The image has three parts a, b and c of which (a.) is the miniaturized gripper imaged using ultrasound in experimental conditions; (b.) is the sample of the belly tissue and (c.) The final dataset that was created by superimposing (a.) over (b)

This was mainly done due to the inability to obtain an dataset by imaging the operation of the gripper in a real-time tissue medium. There were 5 different hydrogel gripper datasets and 4 different types of tissue samples obtained from hand and belly of two different people. The datasets were super imposed as shown in (Fig. 2) to obtain 20 synthetic datasets that were used for the purpose of training and testing. The synthetic datasets were split into 14 training and 6 testing sets. The datasets were carefully split to avoid overfitting. From the training datasets, positive and negative samples of the object to be tracked, in this case the star shaped micro gripper, was collected. There are 300 positive and 1300 negative samples. The size of each positive

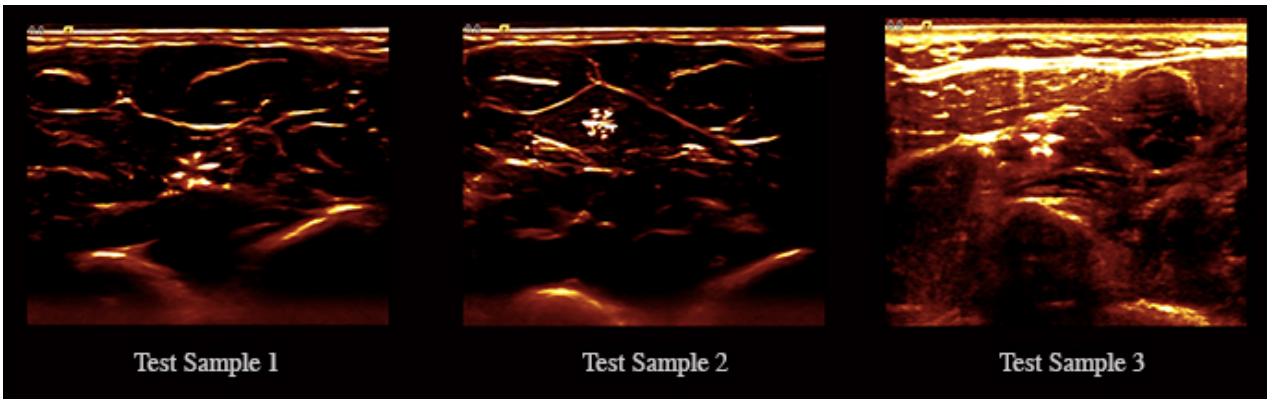

Fig. 3. Snapshots showing an example frame from each test set used for testing the tracker. Test sample 1 has a free moving microgripper superimposed on a belly tissue medium. It video has has 1290 frames. Test sample 2 that is 2193 frames has a micro gripper closing and moving that is superimposed over a similar belly tissue medium. Test sample 3 has 926 frames that has a different free moving gripper super imposed on a tissue sample taken from the forearm.

and negative sample is 90×90 pixels. The positive samples include various orientations and shapes of the miniaturized gripper collected across various different datasets. The negative samples include background and different types of tissue samples except the gripper. Since the obtained image frames only consist of two main colours, it becomes obvious to train the system with the right negative examples so that the classification accuracy of the system increases.

B. Training

The system is trained with HoG and HAAR features using the Adaboost boosting algorithm. For the purpose of training, we use 300 positive and 1300 negative samples. A 20 stage cascade classifier is used to train the system. By altering the values for the negative samples factor *[number of negative samples to be used at every stage of training]* and false alarm rate *[number of negative samples mis classified as positive]* we have different trained models, of which the best is chosen. The training of the HAAR classifier usually takes days together while the training of HoG classifier comparatively takes a lot lesser time. Both the HAAR and HoG classifiers were trained with the same system Mac pro with Ghz processor and 4 GB RAM. The training for HAAR took six and half days, while that for the HoG features, took around 15 hrs. Since the training is done only once, the above mentioned time does not have any significant effect on the overall performance of the classifier.

V. Tests and Results

A. HAAR vs HoG

We have two different classifiers trained using the HAAR and the HoG features. For the purpose of evaluation, groundtruth containing the position of the micro grippers in the test set is made manually. The position values in the groundtruth corresponds to the center of the gripper. The trained classifiers are tested on the test set and the results were tabulated. Error per frame, average error, standard deviation and time taken to process each frame, are calculated and compared for both the classifiers on the same test set.

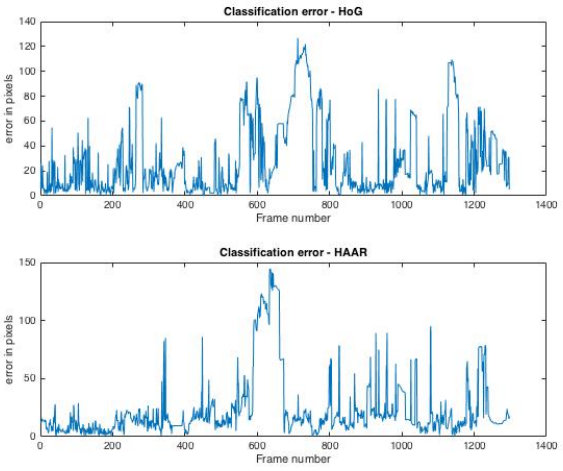

Fig. 4. The classification error per frame, with frame on x-axis and error in y axis. tested against the groundtruth for both HoG and Haar features.

The test set has an interesting mix of complexity. It has three different tissue samples obtained from belly and forearm. The corresponding test samples are named as test 1, test 2 and test 3 as shown in (Fig. 3) where the first two test sets have two different types of belly tissue sample and test 3 has a tissue sample from the forearm respectively. It was observed that the HAAR classifier performed way better with standard deviation of 43 for test sample 1 while HoG performed better with test sample 3 with a standard deviation of 59 pixels. The test sample 3 was relatively tougher to even manually plot the center since in many frames, the micro gripper and the tissue would relatively seem like one. In such a challenging case, when it is difficult to find a HAAR feature, the basic principle of HoG makes it perform better.

B. Tracker implementation

Based on the above obtained results, a tracker was devised combining the effects of cascade classifier, blob exclusion

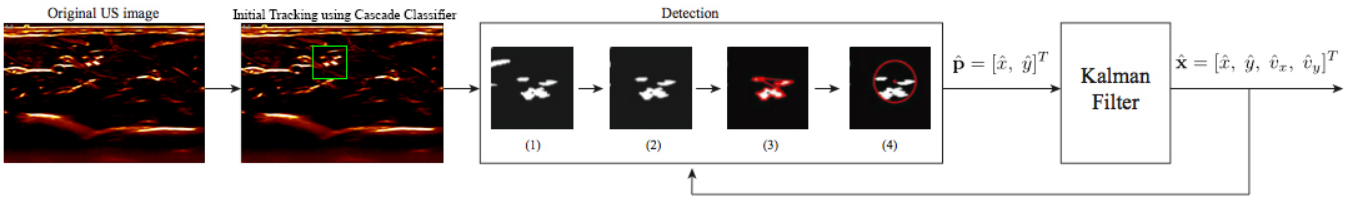

Fig. 5. Flowchart depicting the tracking process: From left to right, a single frame from the synthetic video is taken. The cascade classifier is used for the initial tracking. In the detection phase, based on the initial tracking, a window of 150X150 pixels is considered and only the Red channel of that window is considered. (1) For proper detection of the gripper, a threshold is employed to the window. (2) Small blobs or blobs that are too far from the previous position of the gripper are removed, while merging the remaining adjacent blobs for further consideration. (3) The contours of the segments are computed. (4) A circle fitting is applied on the contour of the segmented area in order to detect the pose p = [$\hat{x}$, $\hat{y}$]^T of the gripper. Finally, state x of the gripper is estimated using a Kalman Filter, where $\hat{v}_x$, $\hat{v}_y$ represent the estimated velocities of the agent. These information are projected back on to the original image. Previously estimated state of the gripper is also used in the current frame to speed up the detection procedure. The scale bar is 4 mm.

based segmentation techniques and a Kalman filter to accurately map the position of the tracker. Both the Haar and HoG features were successfully able to locate the approximate position more than 65-70% of the time, i.e., the gripper is somewhere within the final bounding box, rather being at the center of the box, after the classification. Thus in order to be used for control purposes in real time systems, more accurate localization of the gripper becomes essential. Therefore an algorithm was devised as shown in (Algorithm 1) to solve this problem.

Algorithm 1 Tracker algorithm

function $Tracker(input, output, center, T)$
  $frame \leftarrow GetInputFrame$
  Crop $frame$ to just the information area;
  Apply Cascade classifier on the input $frame$.
  Based on the $output$ of the classifier define a information $window$ in the $frame$.
  Split he obtained $window$ Into RGB;
  Perform BINARY thresholding on R channel;
  Calculate Initial Center using Blob exclusion and Centroid method
  Using a Kalman Filter estimate $center$;
  Display the image back in the RGB channel.
  $output \leftarrow frame$
  Display the center with the frame & save it

Let p = $[\mathbf{x}, \mathbf{y}]^\mathbf{T} \in \mathbb{R}^{\mathbf{2\times1}}$ be the position of a gripper in 2D space and v = $[\mathbf{v_x}, \mathbf{v_y}]^\mathbf{T} \in \mathbb{R}^{\mathbf{2\times1}}$ its velocity. The state of the gripper is defined as x = $[\mathbf{p}, \mathbf{v}] \in \mathbb{R}^{\mathbf{4\times1}}$. Let the miniaturized gripper be considered as a second order system controlled by applying suitable force inputs. The state $\hat{\mathbf{x}}$ of the gripper is estimated during run time by the tracking algorithm. (see Fig. 5). Initially the position $\hat{\mathbf{p}}$ = **[$\hat{\mathbf{x}}$, $\hat{\mathbf{y}}$]**^{T} of the gripper is estimated. In the first step, The RGB image is split into the separate R, G, B channels and only the R channel is considered by the algorithm. Then, binary thresholding is applied to the Red channel. Following it, the connected components concept is applied, wherein small blobs or blobs that are too far from the previous position of the gripper are removed, while merging the remaining adjacent blobs for further consideration. Finally, the contours of the remaining blobs are computed and the centroid of this contour is found out. The estimated position of the gripper $\hat{\mathbf{p}}$ corresponds to the center coordinates of the centroid estimated.

A standard Kalman filter [32] is implemented to consider the second order model of the gripper and control-inputs for estimating the state $\hat{\mathrm{x}}$ from the position estimates $\hat{\mathrm{p}}$. Assuming a constant sampling time Δt of the system, the Kalman filter provides an estimation of the current state $\hat{\mathrm{x}}$ as well as a one-step ahead prediction of $\hat{\mathrm{x}}$. The zero mean multivariate Gaussian distributions N(0,**Q**) and N (0, **R**) are used to estimate the process and measurement noises, respectively, where $\mathbf{Q} \in \mathbb{R}^{4\times4}$ and $\mathbf{R} \in \mathbb{R}^{2\times2}$ are the empirically determined co-variance matrices.

The tracker was tested as before on the same three datasets. The average error was found to be 21 pixels with the HAAR classifier with test set 1 and was found to be 39 pixels for test set 3 with the HOG classifier. The tracking accuracy was greatly improved with an accuracy of over 80%.

VI. Discussion and Conclusion

In order to take the first step towards developing a tracker for tracking the miniaturized gripper inside our body, a special dataset was synthesized with an aim of posing a real tissue like example for a tracker to be trained on. The initial datasets were all imaged under the same conditions, which makes it likely for the gripper to look like the final dataset when injected inside our body. Two different features(HAAR, HoG) were studied on these datasets, in order to utilize the right feature for the purpose of tracking. Based on the initial test results, the final tracker was devised, that had a performance accuracy of nearly 81%. The HAAR classifier performs the best with belly tissue, whereas the HOG's performance with the arm tissue dataset was better. This is due to basic working principle of both the features. HoG works on the orientation of the gradients, which explains how, it was able to work better with the most difficult dataset.

This is an introductory work towards developing a tracker that could accurately map the grippers under any biological

circumstances using ultrasound. As a part of future work, the two features could be combined in a way to use a positive attributes of both the features that could result in one strong feature descriptor. Self thought and deep learning methods would be worked on. Future state predicting estimators such as particle filters would be studied and applied for estimating the position of the gripper, in scenarios of faulty imaging.

REFERENCES

[1] D. Freitag, Using grammatical inference to improve precision in information extraction, in ICML97 Workshop on Automata Induction,Grammatical Inference, and Language Acquisition, Nashville, NT,USA, 1997.

[2] Agarwal, S., Awan, A., and Roth, D. (2004). Learning to detect objects in images via a sparse, part-based representation. IEEE Transactions on Pattern Analysis and Machine Intelligence, 26(11):14751490.

[3] Bensrhair, A., Bertozzi, M., Broggi, A., Miche, P., Mousset, S., and Toulminet, G. (2001). A cooperative approach to vision-based vehicle detection. In Proceedings on Intelligent Transportation Systems, pages 207212.

[4] Bertozzi, M. and Broggi, A. (1997). Vision-based vehicle guidance. Computer, 30(7):4955.

[5] Bertozzi, M., Broggi, A., and Castelluccio, S. (1997). A real-time oriented system for vehicle detection. Journal of Systems Architecture, 43(1-5):317325.

[6] Bucher, T., Curio, C., Edelbrunner, J., Igel, C., Kastrup, D., Leefken, I., Lorenz, G., Steinhage, A., and von Seelen, W. (2003). Image processing and behavior planning for intelligent vehicles. IEEE Transactions on Industrial Electronics, 50(1):6275.

[7] Cha, S. and Srihari, S. N. (2002). On measuring the distance between histograms. Pattern Recognition, 35(6):13551370.

[8] Collado, J., Hilario, C., de la Escalera, A., and Armingol, J. (2004). Model based vehicle detection for intelligent vehicles. In International Symposium on Intelligent Vehicles, pages 572577.

[9] Dellaert, F. (1997). Canss: A candidate selection and search algorithm to initialize car tracking. Technical report, Robotics Institute, Carnegie Mellon University.

[10] Demonceaux, C., Potelle, A., and Kachi-Akkouche, D. (2004). Obstacle detection in a road scene based on motion analysis. IEEE Transactions on Vehicular Technology, 53(6):1649 1656.

[11] Franke, U. (2000). Real-time stereo vision for urban traffic scene understanding. In Proceedings IEEE Intelligent Vehicles Symposium 2000, pages 273278, Detroit, USA.

[12] S. Golemati, J. Stoitsis, G. Emmanouil, T. Balkizas, K. Nikita, Using the Hough transform to segment ultrasound images of longitudinal and transverse sections of the carotid artery,Ultrasound Med Biol 2007, 33(12):1918-1932.

[13] D. Cheng et al, A novel method in detecting CCA lumen diameter and IMT in dynamic B-mode sonography,In 13th International Conference on Biomedical Engineering, vol. 23, pp. 734 737, Berlin, 2009.

[14] R. Benes, J. Karasek, R. Burget, K. Riha, Automatically designed machine vision system for the localization of CCA transverse section in ultrasound images,COMPUTER METHODS AND PROGRAMS IN BIOMEDICINE, 2013, pp. 92-103. ISSN: 0169- 2607.

[15] Z. Weiwei, S. Jian, T. Xiaoou, From Tiger to Panda: Animal Head Detection,IEEE Transactions on Image Processing, 2011

[16] N. Dalal, B. Triggs,Histograms of oriented gradients for human detection,IEEE, Computer Vision and Pattern Recognition, 1990

[17] Y. Ying, W. Han, X. Jian, An automatic system for multi-view face detection and pose estimation,ICARCV, 2010

[18] Freund, Y. and Schapire, R. (1996). Experiments with a new boosting algorithm. In International Conference on Machine Learning, pages 148156.

[19] Friedman, J., Hastie, T., and Tibshirani, R. (2000). Additive logistic regression: a statistical view of boosting. The Annals of Statistics, 28(2):337374.

[20] Gepperth, A., Edelbrunner, J., and Bocher, T. (2005). Realtime detection and classification of cars in video sequences. In Intelligent Vehicles Symposium, pages 625631.

[21] Guo, D., Fraichard, T., Xie, M., and Laugier, C. (2000). Color modeling by spherical influence field in sensing drivingenvironment. In IEEE, editor, Intelligent Vehicles Symposium, pages 249254, Dearborn, MI, USA.

[22] Lowe, D. (1999). Object recognition from local scaleinvariant features. In Proceedings of the International Conference on Computer Vision, pages 11501157.

[23] Papageorgiou, C. and Poggio, T. (1999). A trainable object detection system: Car detection in static images. Technical report, MIT AI Memo 1673 (CBCL Memo 180).

[24] Schneiderman, H. and Kanade, T. (2000). A statistical method for 3d object detection applied to faces and cars. In ICCVPR, pages 746751.

[25] Srinivasa, N. (2002). Vision-based vehicle detection and tracking method for forward collision warning in automobiles. In IEEE Intelligent Vehicle Symposium, volume 2, pages 626631.

[26] Sun, Z., Bebis, G., and Miller, R. (2004). Object detection using feature subset selection. Pattern Recognition, 37(11):21652176.

[27] Sun, Z., Bebis, G., and Miller, R. (2006). On-road vehicle detection: A review. IEEE Trans. Pattern Anal. Mach. Intell., 28(5):694711.

[28] van Leeuwen, M. and Groen, F. (2001). Vehicle detection with a mobile camera. Technical report, Computer Science Institute, University of amsterdam, The Netherlands.

[29] Viola, P. and Jones, M. (2001). Rapid object detection using a boosted cascade of simple features. In Conference on Computer Vision and Pattern Recognition, pages 511518.

[30] Xiong, T. and Debrunner, C. (2004). Stochastic car tracking with line- and color-based features. Advances and Trends in Research and Development of Intelligent Transportation Systems: An Introduction to the Special Issue, 5(4):324328.

[31] Yang, H., Lou, J., Sun, H., Hu, W., and Tan, T. (2001). Efficient and robust vehicle localization. In International Conference on Image Processing, volume 2, pages 355358, Thessaloniki, Greece.

[32] P.R.Belanger, P.Dobrovolny, A.Helmy, and X.Zhang, "Estimation of angular velocity and acceleration from shaft-encoder measurements," The International Journal of Robotics Research, vol. 17, no. 11, pp. 12251233, 1998.

Chapter 5

Discussion

For better understanding, the thesis was split into two major parts. The first part discussed the possibility of using the soft grippers in clinical applications by performing motion control experiments and the second part demonstrated the first step towards developing a tracker for tracking the miniaturized gripper inside our body.

In order to explore new micro-robotic opportunities soft, magnetic micro-robots with shape changing ability was employed and several manipulative tasks were performed using them. To demonstrate its clinical applications, the grippers were imaged and controlled using a clinical imaging modality, ultrasound. In order to show the variety of opportunities with the untethered grippers we started with motion control experiments and performed autonomous motion planning and pick-and-move experiments. These experiments were executed to demonstrate the ability of the grippers to perform such complex manipulation tasks, exploiting its soft properties and approaching more practical purpose in clinical domain.

The motion control experiments consisted of point-to-point motion control and path-following for sine and step trajectory. During these experiments, the gripper was localized and could follow the trajectories (sine and step) with an average positioning error of 0.48 mm with a variance of 0.1 mm. These were the results obtained when the gripper was close to the surface of the water. This condition was essential since the gripper has to have a minimum clearance of atleast 4 mm (thickness of the probe) from the bottom of the container for proper noise-free imaging. This is a little disadvantageous for more complicated and practical experiments which require the folding functionality of the grippers. This is because when the gripper is near the surface, it takes a slightly longer time to close due to the effect of surface tension forces. For our study, sine and step trajectories are the best possible trajectories that could be demonstrated in a magnetic system that could operate in three directions. With the obtained results it is possible

prove that the grippers could be controlled and positioned in two dimensional space to perform manipulative tasks successfully. Also, if this magnetic system is expanded and recreated on a larger scale, there would be enough space to accommodate both the electromagnet and the ultrasound probe, thereby recreating a magnetic control system as demonstrated in [1]. By this way, it is possible to generalize the system for other scenarios.

Results from the motion control experiments show that motion uncertainty, e.g. due to un-modeled external influences on the motion of the agent, or imperfect state information due to partial or noisy measurements of the agents state generates positioning errors. Thus *Linear Quadratic Gaussian Motion Planner* (LQG-MP) was adapted to generate a motion plan which minimized the probability of collisions between the gripper and the environment by considering the motion and sensing uncertainties. The grippers were being autonomously maneuvered through simulated environments with the presence of static obstacles. The gripper was found to assess the environment, simulate upto 30 different paths in 3 seconds and move along the most optimum selected path to reach the target location.

During the pick-and-move experiments 500 m micro-bead was transported for a distance of approximately 14.5 mm with an average velocity of 0.39±0.06 mm/s and positioning error of 0.36±0.05 mm. The experiment was performed out to depict the grasping capabilities of the grippers. Due to the problem with the surface tension forces, the grippers required extra heating to grasp the micro-bead successfully. Also the grippers required strong magnetic field gradients for pulling the gripper with the bead. Patterning the grippers with a higher concentration of iron-oxide would enable the system to apply more magnetic force. Interestingly, the grippers were found to be really sturdy to float near the surface resisting the surface tension forces even after grasping the micro bead. This shows the ability of the grippers to be navigated along the surface of the fluid, that would eliminate most of the obstacles found at the bottom.

In order to take the first step towards developing a tracker for tracking the miniaturized gripper inside our body, a special dataset was synthesized with an aim of posing a real tissue like example for a tracker to be trained on. The initial datasets were all imaged under the same conditions, which makes it likely for the gripper to look like the final dataset when injected inside our body. Two different features (HAAR, HoG) were studied on these datasets, in order to utilize the right feature for the purpose of tracking. Based on the initial test results, the final tracker was devised, that had a performance accuracy of nearly 81%. The HAAR classifier performs the best with belly tissue, whereas the HOG classifier's performance with the arm tissue dataset was better. This is due to basic working principle of both the features. HoG works on the orientation of the

gradients, which explains how, it was able to work better with the most difficult dataset.

Chapter 6

Conclusion

So far we have seen and exploited the miniaturized grippers shape changing ability to pick and move objects using ultrasound images. This is by far the first attempt towards taking these miniaturized grippers towards using them in clinical bio-medical applications. The motion planning and control experiments resulted with an almost equivalent results as controlled using digital camera feedback. The difference in the results is attributed to the worse resolution of the obtained US images. This we believe is a small step towards using these micro agents in untethered surgical operations.

The motion experiments along with pick and move has less than 0.5 mm average positioning error that is a great sign for successful utilization of these grippers in variety of clinical applications. The initial study on developing a tracker mimicking these miniaturized grippers operation in real tissue environment has also interesting insights that could lead to significant contribution to the scientific community. The comparison of HAAR and HoG features to be used in combination with object tracking using ultrasound images is also another important contribution of this thesis.

As a part of future work, three dimensional tracking and control of the grippers would be studied. Visualizing and controlling the micro grippers using current VR/AR (Virtual Reality/Augmented Reality)and haptic modalities would also be studied. An improved heating and cooling system for a quicker cooling and heating to perform more sophisticated open and close scenarios would be developed. Moreover, advanced control techniques (e.g., cascade control) will be used to optimize the tracking of more intricate paths. Further-more, motion control and planning of miniaturized grippers will be achieved in fluidic micro-channels with time-varying flow rates based on the feedback provided by the ultrasound system.

Bibliography

[1] F. Ongaro et al., "Control of untethered soft grippers for pick-and-place tasks," 2016 6th IEEE International Conference on Biomedical Robotics and Biomechatronics (BioRob), Singapore, 2016, pp. 299-304.

[2] S. Martel and M. Mohammad, "Using a swarm of self-propelled natural microrobots in the form of flagellated bacteria to perform com- plex micro-assembly tasks," in Proceedings of the IEEE International Conference on Robotics and Automation (ICRA), pp. 500505, Alaska, USA, May 2010.

[3] S.Tottori,L.Zhang,F.Qiu,K.K.Krawczyk,A.Franco-Obrego n,and B. J. Nelson, "Magnetic helical micromachines: fabrication, controlled swimming, and cargo transport," Advanced materials, vol. 24, no. 6, pp. 811816, 2012.

[4] M.Sitti,H.Ceylan,W.Hu,J.Giltinan,M.Turan,S.Yim,andE.Diller, "Biomedical applications of untethered mobile milli/microrobots," Proceedings of the IEEE, vol. 103, no. 2, pp. 205224, 2015.

[5] J. S. Randhawa, T. G. Leong, N. Bassik, B. R. Benson, M. T. Jochmans, and D. H. Gracias, "Pick-and-place using chemically actu- ated microgrippers," Journal of the American Chemical Society, vol. 130, no. 51, pp. 17 23817 239, 2008.

[6] E. Diller and M. Sitti, "Three-dimensional programmable assembly by untethered magnetic robotic micro-grippers," Advanced Functional Materials, vol. 24, no. 28, pp. 43974404, 2014.

[7] A. Ichikawa, S. Sakuma, F. Arai., and S. Akagi, "Untethered micro- robot with gripping mechanism for on-chip cell surgery utilizing outer magnetic force," in Proceedings of the IEEE International Conference on Robotics and Automation (ICRA), pp. 37953800, Hong Kong, China, May 2014.

[8] K. Malachowski, M. Jamal, Q. Jin, B. Polat, C. J. Morris, and D. H. Gracias, "Self-folding single cell grippers," Nano Letters, vol. 14, no. 7, pp. 41644170, 2014.

[9] S. Sanchez, A. A. Solovev, S. Schulze, and O. G. Schmidt, Controlled manipulation of multiple cells using catalytic microbots, Chemical Communications, vol. 47, no. 2, pp. 698 700, 2011.

[10] I. S. Khalil, F. van den Brink, O. S. Sukas, and S. Misra, Microassembly using a cluster of paramagnetic microparticles, in Robotics and Automation (ICRA), 2013 IEEE International Conference on, pp. 55275532, IEEE, 2013.

[11] S.MartelandM.Mohammadi,Usingaswarmofself-propelled natural microrobots in the form of flagellated bacteria to perform complex micro-assembly tasks, in Robotics and Automation (ICRA), 2010 IEEE International Conference on, pp. 500505, IEEE, 2010.

[12] S. R. Platt, J. Hawks, M. E. Rentschler, et al., Vision and task assistance using modular wireless in vivo surgical robots, Biomedical Engineering, IEEE Transactions on, vol. 56, no. 6, pp. 17001710, 2009.

[13] K. Harada, D. Oetomo, E. Susilo, A. Menciassi, D. Daney, J.-P. Merlet, and P. Dario, A reconfigurable modular robotic endoluminal surgical system: vision and preliminary results, Robotica, vol. 28, no. 02, pp. 171183, 2010.

[14] A. C. Lehman, N. A. Wood, S. Farritor, M. R. Goede, and D. Oleynikov, Dexterous miniature robot for advanced min- imally invasive surgery, Surgical endoscopy, vol. 25, no. 1, pp. 119123, 2011.

[15] N. Bassik, B. T. Abebe, K. E. Laflin, and D. H. Gracias, Photolithographically patterned smart hydrogel based bilayer actuators, Polymer, vol. 51, no. 26, pp. 60936098, 2010.

[16] C. Yoon, R. Xiao, J. Park, J. Cha, T. D. Nguyen, and D. H. Gracias, Functional stimuli responsive hydrogel devices by self-folding, Smart Materials and Structures, vol. 23, no. 9, p. 094008, 2014.

[17] K. Malachowski, M. Jamal, Q. Jin, B. Polat, C. J. Morris, and D. H. Gracias, Self-folding single cell grippers, Nano letters, vol. 14, no. 7, pp. 41644170, 2014.

[18] M. Jamal, A. M. Zarafshar, and D. H. Gracias, Differentially photo-crosslinked polymers enable self-assembling microflu- idics, Nature communications, vol. 2, p. 527, 2011.

[19] S. Martel, O. Felfoul, J.-B. Mathieu, A. Chanu, S. Tamaz, M. Mo- hammadi, M. Mankiewicz, and N. Tabatabaei. MRI-based medical nanorobotic platform for the control of magnetic nanoparticles and flagellated bacteria for target interventions in human capillaries. Int. J. of Robotic Research, 28(9):11691182, 2009.

[20] J.-B. Mathieu and S. Martel. Steering of aggregating magnetic microparticles using propulsion gradients coils in an MRI scanner. Magnetic Resonance in Medicine, 63(5):13361345, 2010.

[21] B. J. Nelson, I. K. Kaliakatsos, and J. J. Abbott. Microrobots for minimally invasive medicine. Annual Review of Biomedical Engineering, 12:5585, 2010.

[22] E. Gultepe, J. S. Randhawa, S. Kadam, S. Yamanaka, F. M. Selaru, E. J. Shin, A. N. Kalloo, and D. H. Gracias, "Biopsy with thermally- responsive untethered microtools," Advanced Materials, vol. 25, no. 4, pp. 514519, 2012.

[23] J. S. Randhawa, K. E. Laflin, N. Seelam, and D. H. Gracias, "Microchemomechanical systems," Advanced Functional Materials, vol. 21, no. 13, pp. 23952410, 2011.

[24] K. Malachowski, J. Breger, H. R. Kwag, M. O. Wang, J. P. Fisher, F. M. Selaru, and D. H. Gracias, "Stimuli-responsive theragrippers for chemomechanical controlled release," Angewandte Chemie, vol. 126, no. 31, pp. 81838187, 2014.

[25] S. Fusco, M. S. Sakar, S. Kennedy, C. Peters, R. Bottani, F. Starsich, A. Mao, G. A. Sotiriou, S. Pane , S. E. Pratsinis et al., "An integrated microrobotic platform for on-demand, targeted therapeutic interven- tions," Advanced Materials, vol. 26, no. 6, pp. 952957, 2014.

[26] S. Fusco, M. S. Sakar, S. Kennedy, C. Peters, S. Pane, D. Mooney, and B. J. Nelson, "Self-folding mobile microrobots for biomedical applications," in Proceedings of the IEEE International Conference on Robotics and Automation (ICRA), pp. 37773782, Hong Kong, China, 2014.

[27] J. C. Kuo, H. W. Huang, S. W. Tung, and Y. J. Yang, "A hydrogel- based intravascular microgripper manipulated using magnetic fields," Sensors and Actuators A: Physical, vol. 211, pp. 121130, 2014.

[28] S. Miyashita, S. Guitron, M. Ludersdorfer, C. R. Sung, and D. Rus, "Untethered miniature origami robot that self-folds, walks, swims, and degrades," in Proceedings of the IEEE International Conference on Robotics and Automation (ICRA), pp. 14901496, Seattle, WA, USA, May 2015.

[29] H.Li,G.Go,S.Y.Ko,J.-O.Park,andS.Park,"Magneticactuatedph- responsive hydrogel-based soft micro-robot for targeted drug delivery," Smart Materials and Structures, vol. 25, no. 2, p. 027001, 2016.

[30] D. H. Gracias, "Stimuli responsive self-folding using thin polymer films," Current Opinion in Chemical Engineering, vol. 2, no. 1, pp. 112119, 2013.

[31] J. C. Breger, C. Yoon, R. Xiao, H. R. Kwag, M. O. Wang, J. P. Fisher, T. D. Nguyen, and D. H. Gracias, "Self-folding thermo-magnetically responsive soft microgrippers," ACS Applied Materials & Interfaces, vol. 7, no. 5, pp. 33983405, 2015.

[32] A. Sanchez, Y. M. Sadek, I. S. M. Khalil, and S. Misra, "Mobi- mag: A compact device for medical research using wireless control of magnetic microrobots," in Proceedings of the Design of Medical Devices Conference-Europe, pp. 100101, Delft, Netherlands, October 2014.

[33] G. F. Franklin, J. D. Powell, and A. Emami-Naeini, "Feedback control of dynamics systems," Addison-Wesley, Reading, MA, 1994.

[34] A. S. Bahaj, P. A. B. James, and F. D. Moeschler, "An alternative method for the estimation of the magnetic moment of non-spherical magnetotactic bacteria," IEEE Transactions on Magnetics, vol. 32, no. 5, pp. 51335135, 1996.

[35] Y.R.Chemla,H.L.Grossman,T.S.Lee,J.Clarke,M.Adamkiewicz, and B. B. Buchanan, "A new study of bacterial motion: superconducting quantum interference device microscopy of magnetotactic bacteria," Biophysical Journal, vol. 76, no. 6, pp. 33233330, 1999.

[36] W. F. Brown, "Magnetostatic principles," in Ferromagnetism. North- Holland Amsterdam, 1962.